Supporting Information for

Ubiquinone-BODIPY Nanoparticles for Tumor Redox-Responsive Fluorescence Imaging and Photodynamic Activity

Byunghee Hwang,[a] Tae-Il Kim,[a] Hyunjin Kim,[b] Sungjin Jeon,[a] Yongdoo Choi*[b] and Youngmi Kim*[a]

[a]*Department of Chemistry and Research Institute of Basic Sciences, Kyung Hee University, 26 Kyungheedae-ro, Dongdaemun-gu, Seoul, 02447, Korea.*
[b]*Molecular Imaging & Therapy Branch, National Cancer Center, 323 Ilsan-ro, Goyang-si, Gyeonggi-do, 10408, Korea*

youngmi.kim@khu.ac.kr
Tel: +82 2-961-9537
Fax: +82 2-961-0443

ydchoi@ncc.re.kr
Tel: +82 31-920-2512
Fax: +82 31-920-2529

Table of Contents

1. Synthesis of Compounds **S3**
2. Photophysical Property Studies **S6**
3. Self-Assembled Aggregate Formation of **PS-Q** Conjugate in PBS buffer **S8**
4. Properties of **PS-A** **S11**
5. Evaluation of Singlet Oxygen ($^1O_2$) Generation Efficiency **S13**
6. GSH-Induced Fluorescence Activation of **PS-Q-NP** **S19**
7. Two Plausible Mechanisms for "Turn-on" Fluorescence and Photosensitizing Activities **S24**
8. Confirmation of **PS-Q-NP** to **PS-A** Conversion by LC-MS Analysis **S25**
9. Cell Studies **S27**
10. *In vivo* Studies **S28**
11. ^{1}H-NMR and ^{13}C-NMR Spectra **S29**
12. References **S34**

Experimental

Materials

All chemicals were of reagent grade quality, purchased commercially, and used as received without further purification unless otherwise noted. Anhydrous toluene, ethyl acetate, CH_3CN, CH_2Cl_2 and DMF were obtained as sure-seal bottles from Alfa Aesar. 1,1′,3,3,3′,3′-Hexamethylindotricarbocyanine iodide, *N*-bromosuccinimide (NBS), *N*-iodosuccinimide (NIS), triphenylphosphine, oxidized glutathione (GSSG), human NAD(P)H:quinone oxidoreductase isozyme 1 (hNQO1, EC 1.6.5.2, 100 U/mg), reduced nicotinamide adenine dinucleotide (NADH), homocysteine, porcine liver esterase (PLE, EC 3.1.1.1, 17 U/mg), trypsin from porcine pancreas (EC 3.4.21.4, 1000-2000 U/mg), lipase from porcine pancreas (PPL, EC 3.1.1.3, 100-500 U/mg), bovine serum albumin (BSA), KO_2 and *tert*-butyl hydroperoxide (TBHP) were purchased from Aldrich (Saint Louis, MO). Reduced glutathione (GSH), cysteine, lysine, serine, glucose, and 1,3-diphenylisobenzofuran (DPBF) were purchased TCI Co., Ltd. (Tokyo, Japan). Hydrogen peroxide (H_2O_2) and sodium hypochlorite (NaOCl) were purchased from Samchun Chemicals (Korea). Singlet Oxygen Sensor Green® (SOSG) was purchased from ThermoFisher Scientific Co. (Waltham, MA). Flash column chromatography was performed using silica gel (38−75 μm), which was supplied from Qingdao Meigao Chem. Co., Ltd (Chengyang, China). Aqueous solutions were freshly prepared with deionized water from a water purification system (Younglin. Korea). Compounds **1**,[1] **3a**,[2] and 3,4-bis[2-[2-(2-methoxyethoxy)ethoxy]ethoxy]benzaldehyde[3] were prepared as described in the literature.

General methods, instrumentation and measurements

Synthetic manipulations that required an inert atmosphere (where noted) were carried out under a nitrogen using standard Schlenk techniques. NMR (^{1}H, ^{13}C) spectra were recorded on Bruker Avance 400 MHz spectrometer. The ^{1}H and ^{13}C chemical shifts (δ) were reported in units of parts per million (ppm), referenced to the residual solvent. Splitting patterns are denoted as s (singlet), d (doublet), t (triplet), q (quartet), m (multiplet), and br (broad). High-resolution electrospray ionization (ESI) mass spectra were obtained at the Korean National Center for Inter-University Research. UV-Vis absorption spectra were obtained on a SCINCO S-3100 spectrophotometer. Fluorescence measurements were recorded on a Hitachi F-7000 fluorescence spectrophotometer using quartz cuvettes with a path length of 1 cm. Continuous wave (CW) laser with 670 nm wavelength was purchased from Laser lab (Anyang, Korea). Fluorescence quantum yields were determined using 1,1′,3,3,3′,3′-hexamethylindotricarbocyanine iodide (HITCI, Φ_{FL} = 0.28 in MeOH)[4] and cresyl violet (Φ_{FL} = 0.56 in EtOH)[5] as standards. Particle size was measured by dynamic light scattering (DLS) using a Malvern particle analyzer ZEN1690. Scanning electron microscopy (SEM) images were obtained from a Carl Zeiss Sigma microscope operating at an accelerating voltage of 5.0 kV (Oberkochen, Germany). Absorption and fluorescence emission spectra recorded in assays were obtained using a Synergy H1 Microplate Reader (BioTek, USA).

1. Synthesis of Compounds

(a) Synthesis of compounds PS-E, PS-A, and PS-Q

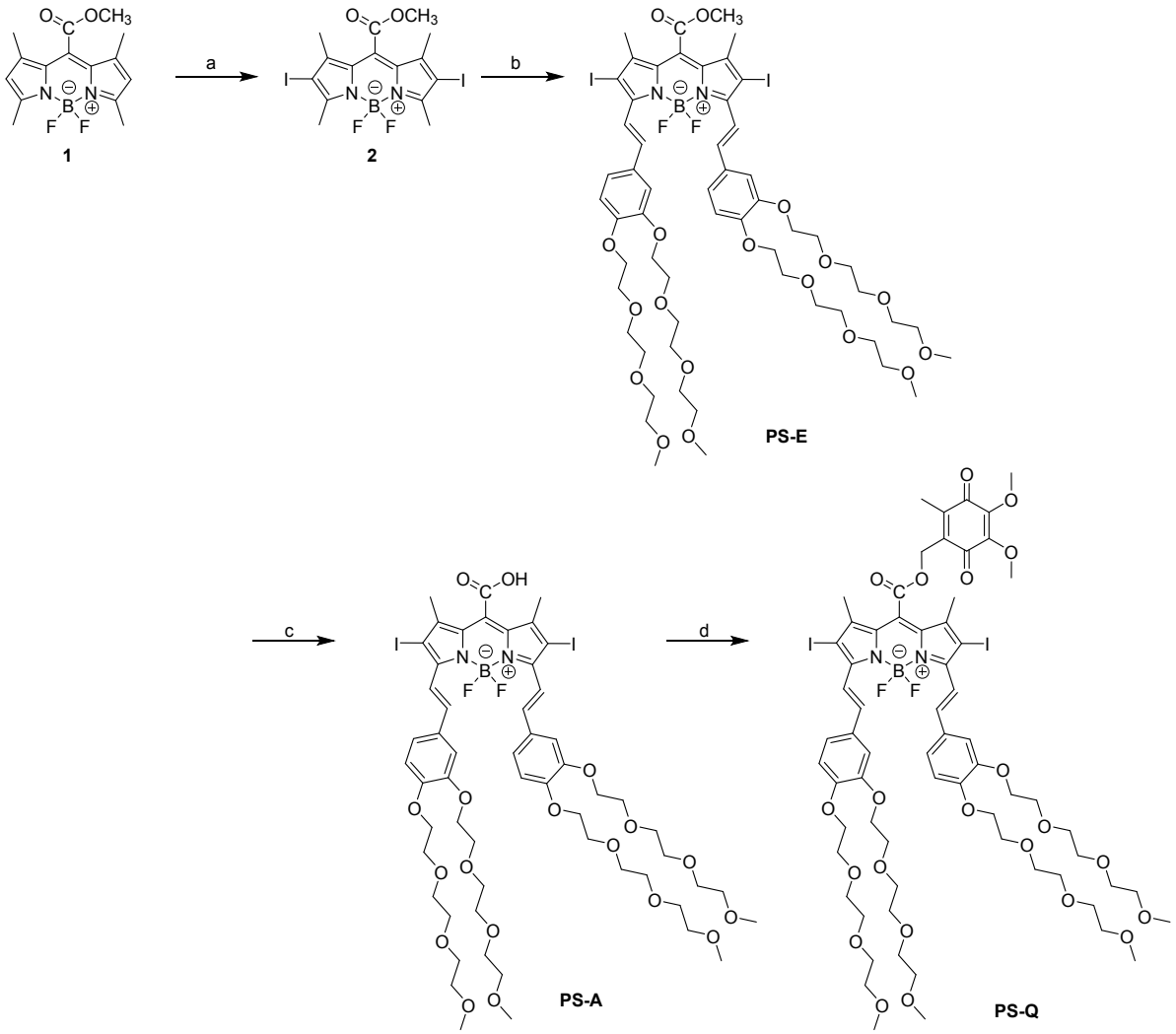

Scheme S1. Synthetic scheme for compounds, reagents and conditions. (a) *N*-iodosuccinimide (NIS), dry CH_2Cl_2, room temperature, overnight, 90%; (b) 3,4-bis[2-[2-(2-methoxyethoxy)ethoxy]ethoxy]benzaldehyde,[3] piperidine, CH_3COOH, dry toluene, 80 °C, 4 h, 40%; (c) LiI, dry ethyl acetate, 100 °C, 16 h, 70% (d) **4**, K_2CO_3, dry DMF, room temperature, 4 h, 50%.

Compound **2**. To a stirred solution of compound **1**[1] (100 mg, 0.32 mmol) in dry CH_2Cl_2 (10 mL) at room temperature under a nitrogen atmosphere was added *N*-iodosuccinimide (287 mg, 1.28 mmol). After stirring at room temperature for overnight, the reaction solvent was removed under reduced pressure, and the crude product was purified by column chromatography on silica gel using progressively more polar 10:1 to 1:1 hexanes:dichloromethane as the mobile phase to afford compound **2** as a khaki-gold solid (164 mg, 90%). ^{1}H-NMR (400 MHz, $CDCl_3$): δ = 4.00 (s, 3H), 2.62 (s, 6H), 2.13 (s, 6H). ^{13}C-NMR (100 MHz, $CDCl_3$): δ = 165.3, 158.9, 143.5, 128.4, 128.2, 85.6, 53.5, 16.2, 15.1. HR-MS (ESI) calcd. for $C_{15}H_{15}BF_2N_2O_2I_2Na$ $[M+Na]^+$: 580.9178; found 580.9182.

Compound **PS-E**. To a stirred solution of compound **2** (100 mg, 0.18 mmol) and 3,4-bis[2-[2-(2-methoxyethoxy)ethoxy]ethoxy]benzaldehyde[3] (231 mg, 0.54 mmol) in dry toluene (7 mL) at room temperature under a nitrogen atmosphere was added piperidine (200 μL, 1.8 mmol) and acetic acid (120 μL, 1.8 mmol). After stirring at 80 °C for 4 hours, the resulting mixture was cooled to room temperature. Then, the mixture was diluted with ethyl acetate (100 mL) and washed three times with water (50 mL × 3). The collected organic layers were dried over dry $MgSO_4$, filtered, and evaporated under reduced pressure. The crude product was purified by column chromatography on silica gel using progressively more polar 100:1 to 20:1 dichloromethane:methanol as the mobile phase to afford compound **PS-E** as a dark green solid (99 mg, 40%).
^{1}H- NMR (400 MHz, $CDCl_3$): δ = 8.12 (d, *J*=16.4 Hz, 2H), 7.48 (d, *J*=16.4 Hz, 2H), 7.29 (d, *J*=8 Hz, 2H), 7.15 (s, 2H), 6.96 (d, *J*=8 Hz 2H), 4.24 (d, *J*=4 Hz, 8H), 4.01 (s, 3H), 3.89 (d, *J*=3.6 Hz, 8H), 3.76 (s, 8H), 3.68 (d, *J*=4 Hz, 16H), 3.54 (d, *J*=4.4 Hz, 8H), 3.37 (s, 6H), 3.34 (s, 6H), 2.20 (s, 6H). ^{13}C-NMR (100 MHz, $CDCl_3$): δ = 165.8, 151.6, 150.4, 148.6, 143.5, 140.2, 130.3, 130.2, 125.2, 122.1, 116.9, 114.2, 114.1, 71.8, 70.6, 70.4, 69.5, 69.4, 68.9, 68.5, 59.1, 15.5. HR-MS (ESI) calcd. for $C_{57}H_{79}N_2O_{18}F_2BI_2Na$ $[M+Na]^+$: 1405.3401; found 1405.3376.

Compound **PS-A**. To a stirred solution of **PS-E** (50 mg, 0.036 mmol) in dry ethyl acetate (5 mL) at room temperature under a nitrogen atmosphere was added LiI (10 mg, 0.072 mmol). The resulting mixture was refluxed at 100 °C for 16 hours. After the reaction was complete, the reaction mixture was cooled to room temperature. Then, the mixture was diluted with ethyl acetate (50 mL) and washed with 1 M HCl solution (50 mL × 3). The combined organic layers were dried over dry $MgSO_4$, filtered, and evaporated under reduced pressure. The crude product was purified by column chromatography on silica gel using progressively more polar 20:1 to 5:1 dichloromethane:methanol as the mobile phase to afford **PS-A** as a blue solid (34 mg, 70%).
^{1}H-NMR (400 MHz, CD_3OD): δ = 8.09 (d, *J*=16.4 Hz, 2H), 7.51 (d, *J*=16.8 Hz, 2H), 7.25 (s, 2H), 7.22 (d, *J*=8 Hz, 2H), 7.03 (d, *J*=8.4 Hz, 2H), 4.24 (d, *J*=4.4 Hz, 8H), 3.85 (m, 8H), 3.69 (m, 8H), 3.61 (m, 16H), 3.48 (m, 8H), 3.32 (s, 12H), 2.49 (s, 6H). ^{13}C-NMR (100 MHz, CD_3OD): δ = 149.9, 149.3, 148.5, 144.4, 137.8, 130.4, 129.2, 121.6, 117.0, 113.6, 112.6, 71.4, 71.3, 70.1, 69.9, 69.8, 69.7, 69.1, 68.9, 68.5, 68.1, 57.7, 14.6. HR-MS (ESI): calcd. for $C_{56}H_{77}N_2O_{18}F_2BI_2Na$ $[M+Na]^+$: 1391.3247; found 1391.3220.

Compound **PS-Q** conjugate. To a stirred solution of **PS-A** (30 mg, 0.021 mmol) and K_2CO_3 (9.1 mg, 0.063 mmol) in dry DMF (3 mL) at room temperature under a nitrogen atmosphere was added a solution of 2-bromomethyl-5,6-dimethoxy-3-methyl-[1, 4]benzoquinone **4** (18 mg, 0.063 mmol) in dry DMF (3 mL). The resulting mixture was stirred at room temperature for 4 hours. After the reaction was complete, the reaction solvent was evaported under reduced pressure, and the crude product was purified by column chromatography on silica gel using progressively more polar 100:1 to 20:1 dichloromethane:methanol as the mobile phase to afford **PS-Q** conjugate as a dark green solid (16.4 mg, 50%).
^{1}H-NMR (400 MHz, $CDCl_3$): δ = 8.11 (d, *J*=16.4 Hz, 2H), 7.47 (d, *J*=16.8 Hz, 2H), 7.28 (d, 2H), 7.14 (s, 2H), 6.95 (d, *J*=8.4 Hz, 2H), 5.26 (s, 2H), 4.24 (d, *J*=4.4 Hz, 8H), 4.05 (s, 3H), 4.00 (s, 3H), 3.89 (d, *J*=4.4 Hz, 8H), 3.71 (m, 8H), 3.65 (m, 16H), 3.53 (m, 8H), 3.37 (s, 6H), 3.35 (s, 6H), 2.29 (s, 6H), 2.19 (s, 3H). ^{13}C-NMR (100 MHz, $CDCl_3$): δ = 183.6, 182.4, 170.6, 165.1, 151.8, 150.6, 148.8, 144.8, 143.6, 140.4, 138.1, 130.3, 130.2, 124.3, 122.1, 116.9, 114.2, 114.1, 83.2, 71.8, 70.7, 70.5, 70.4, 69.6, 69.4, 69.0, 68.6, 61.4, 59.3, 59.1, 59.0, 29.7, 21.1, 15.7, 12.6. HR-MS (ESI): calcd. for $C_{66}H_{87}N_2O_{22}F_2BI_2Na$ $[M+Na]^+$: 1585.3806; found 1585.3799.

(b) Synthesis of compound 4

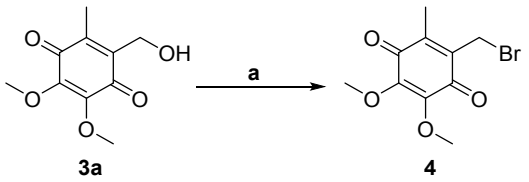

Scheme S2. Synthetic scheme for 2-bromomethyl-5,6-dimethoxy-3-methyl-[1, 4]benzoquinone **4**, reagents and conditions. (a) *N*-bromosuccinimide (NBS), triphenylphosphine, dry CH_3CN, room temperature, 2 h, 50%.

2-Bromomethyl-5,6-dimethoxy-3-methyl-[1, 4]benzoquinone **4**. To a stirred solution of compound **3a**[2] (240 mg, 1.13 mmol) in dry CH_3CN (5 mL) at room temperature under a nitrogen atmosphere was added *N*-bromosuccinimide (402 mg, 2.26 mmol) and triphenylphosphine (593 mg, 2.26 mmol). After stirring at room temperature for 2 hours, the reaction solvent was removed under reduced pressure. The crude compound was diluted with CH_2Cl_2 (50 mL) and washed three times with water (100 mL × 3). The collected organic layers were dried over dry $MgSO_4$, filtered, and evaporated under reduced pressure. The crude product was purified by column chromatography on silica gel using progressively more polar 50:1 to 10:1 hexanes:ethyl acetate as the mobile phase to afford compound **4** as a reddish oil (157.3 mg, 50%).
^{1}H-NMR (400 MHz, $CDCl_3$): δ = 4.24 (s, 2H), δ = 3.96 (s, 3H), 3.94 (s, 3H), 2.03 (s, 3H). ^{13}C-NMR (100 MHz, $CDCl_3$): δ 182.8, 180.6, 143.9, 143.4, 140.7, 136.5, 60.4, 60.3, 20.5, 11.0. HR-MS (ESI): calcd. for $C_{10}H_{11}O_4BrNa$ $[M+Na]^+$: 296.9734; found 296.9738.

2. Photophysical Property Studies

Table S1. Photophysical properties of compounds

Compounds	Solvent	$\lambda_{abs.\ max}$ [nm]	ε^b [$M^{-1}cm^{-1}$]	$\lambda_{em.\ max}{}^c$ [nm]	Φ_{FL}
PS-Q	DMSO	711	95,000	756	0.003[d]
PS-Q	Buffer[a]	669/716	n/a	751	0.0001[d]
PS-E	DMSO	703	98,000	767	0.008[d]
PS-E	Buffer[a]	657	n/a	750	0.0003[d]
PS-A	DMSO	633	75,000	675	0.15[e]
PS-A	Buffer[a]	648	n/a	691	0.01[e]

[a]In 10 mM phosphate buffered saline solution (PBS, pH 7.4, 1% DMSO). [b]Measured at each absorption maximum. [c]Excited at 600 nm. [d]Quantum yields vs. 1,1′,3,3,3′,3′-Hexamethylindotricarbocyanine iodide (Φ_{FL} = 0.28 in MeOH).[4] [e]Quantum yields vs. Cresyl violet (Φ_{FL} = 0.56 in EtOH).[5] n/a: not available.

(a) Absorption and fluorescence emission spectra of compounds in DMSO

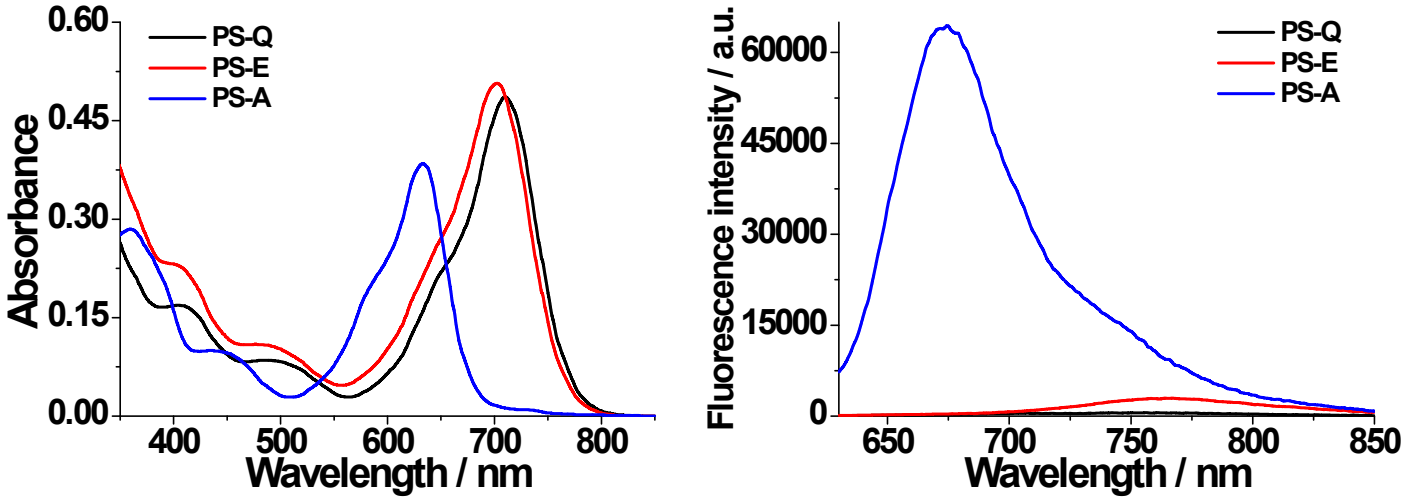

Figure S1. Absorption (left) and fluorescence emission (right) spectra of **PS-Q (**black lines), **PS-E** (red lines), and **PS-A** (blue lines) in DMSO at 25 °C. Excited at 600 nm. [**PS-Q**] = [**PS-E**] = [**PS-A**] = 5 μM.

(b) Absorption and fluorescence emission spectra of compounds in PBS buffer

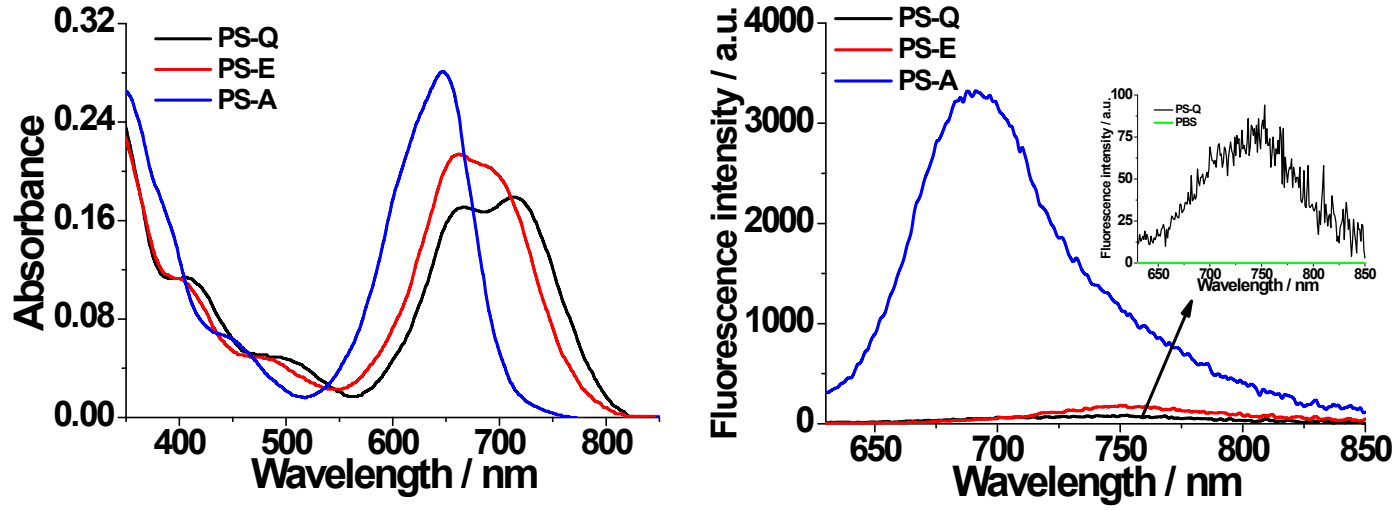

Figure S2. Absorption (left) and fluorescence emission (right) spectra of **PS-Q (**black lines), **PS-E** (red lines), and **PS-A** (blue lines) in PBS (10 mM, pH 7.4, 1% DMSO) at 25 °C. Excited at 600 nm. [**PS-Q**] = [**PS-E**] = [**PS-A**] = 5 μM. Inset shows fluorescence emission spectra of **PS-Q-NPs** (black) and PBS buffer only (10 mM, pH 7.4, 1% DMSO, green).

3. Self-Assembled Aggregate Formation of PS-Q Conjugate in PBS buffer

(a) Identification of the formation of nanoparticles (PS-Q-NP) from PS-Q conjugate

Additional Scanning Electron Microscope (SEM) images of ***PS-Q-NP***

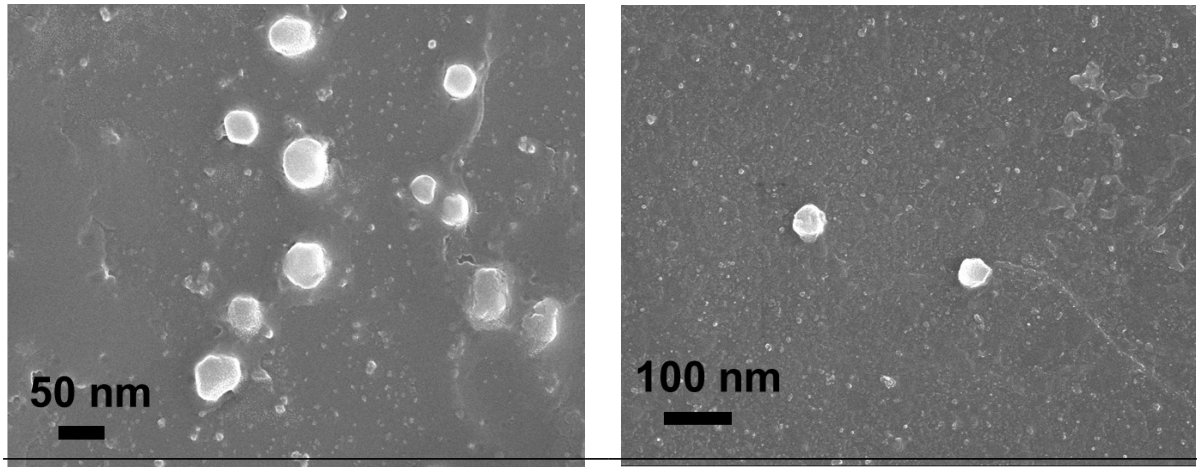

Figure S3. SEM images of the dried **PS-Q-NP**, formed from a solution of **PS-Q** conjugate (5 μM) in water-DMSO (99:1, v/v) at 25 °C. Size = 45 ± 5 nm.

Dynamic Light Scattering (DLS) analysis of ***PS-Q-NP***

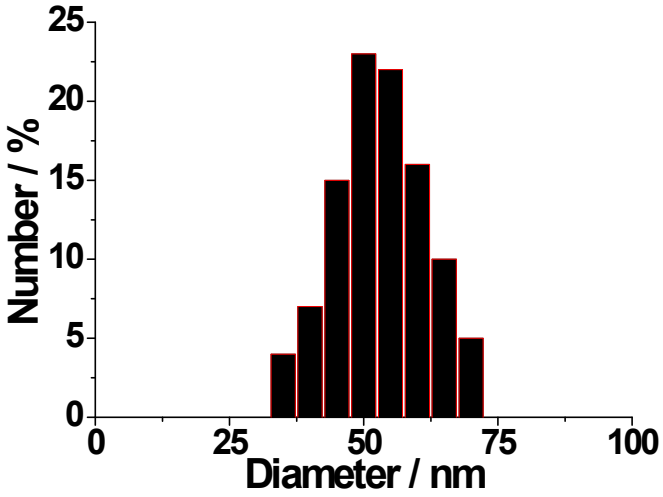

Figure S4. Particle size distribution of **PS-Q-NP**, prepared from **PS-Q** conjugate (5 μM) in PBS buffer (10 mM, pH 7.4, 1% DMSO) at 25 °C. The size was measured immediately after the addition of **PS-Q** conjugate (in DMSO) into PBS (10 mM, pH 7.4) at 25 °C. Average diameter = 50 ± 12 nm.

(b) Stability of colloidal PS-Q-NP in PBS buffer

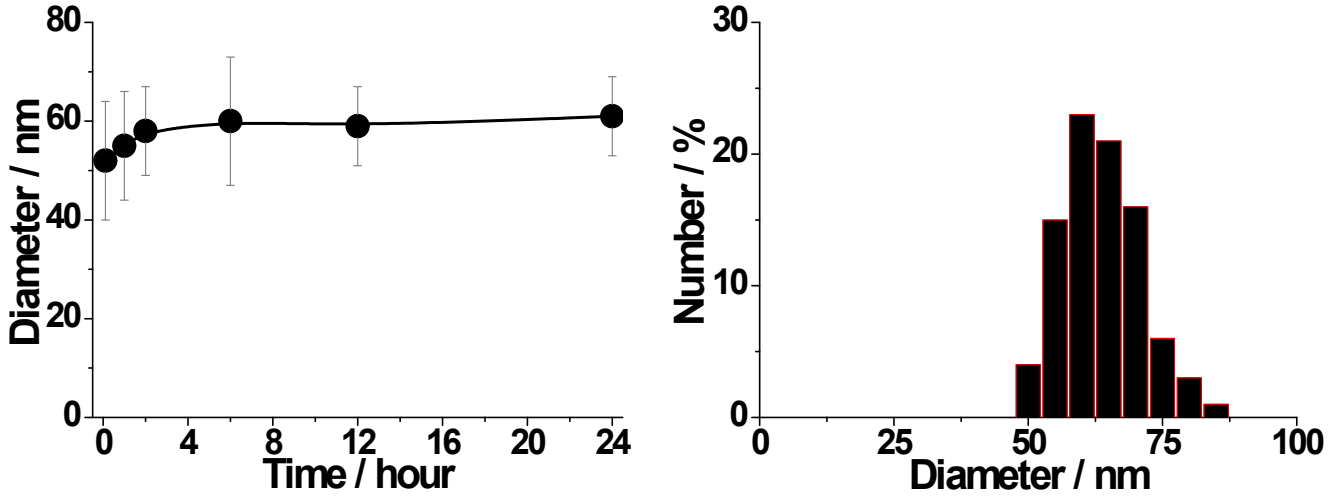

Figure S5. (left) Monitoring size of **PS-Q-NP** (5 μM) as a function of incubation time (0, 1, 2, 6, 12, 24 hours) under dark conditions in PBS (10 mM, pH 7.4, 1% DMSO) at 25 °C. (right). Particle size distribution of **PS-Q-NP** after incubation in PBS buffer (10 mM, pH 7.4, 1% DMSO) for 24 hours. **PS-Q-NP** was prepared from **PS-Q** conjugate (5 μM) in PBS (10 mM, pH 7.4, 1% DMSO) at 25 °C. Average diameter = 61 ± 15 nm.

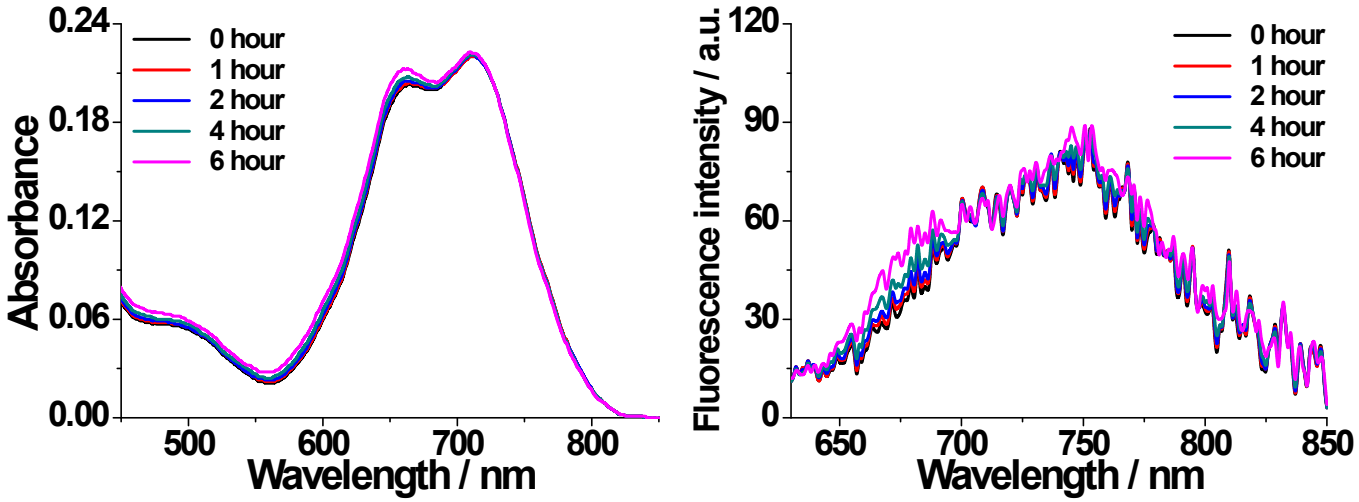

Figure S6. Chemical stability of **PS-Q-NP**. Time-dependent absorption (left) and fluorescence emission (right) spectra of **PS-Q-NP** (5 μM) in PBS (10 mM, pH 7.4, 1% DMSO) at 25 °C. All spectra were obtained during incubation for 6 hours under dark conditions. Excited at 600 nm. Negligible changes in absorption and emission spectra of **PS-Q-NP** were observed, indicating that **PS-Q-NP** is highly stable against non-specific hydrolysis and well-dispersed in aqueous buffer solution.

(c) Effect of pH on absorption and emission spectra of PS-Q-NP (before and after 12 h incubation)

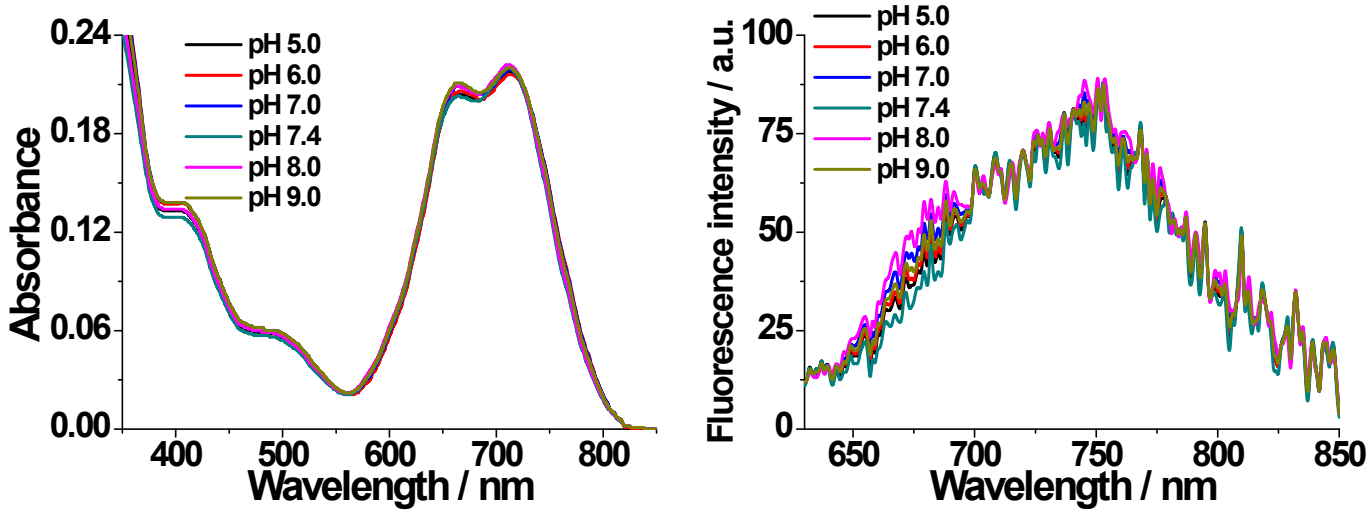

Figure S7. Absorption (left) and fluorescence emission (right) spectra of **PS-Q-NP** (5 μM) in different pH (pH 5–9) buffer systems containing 1% DMSO as a cosolvent at 25 °C. Excited at 600 nm. The spectra was recorded immediately after the addition of **PS-Q** conjugate (in DMSO) into each buffer solution.

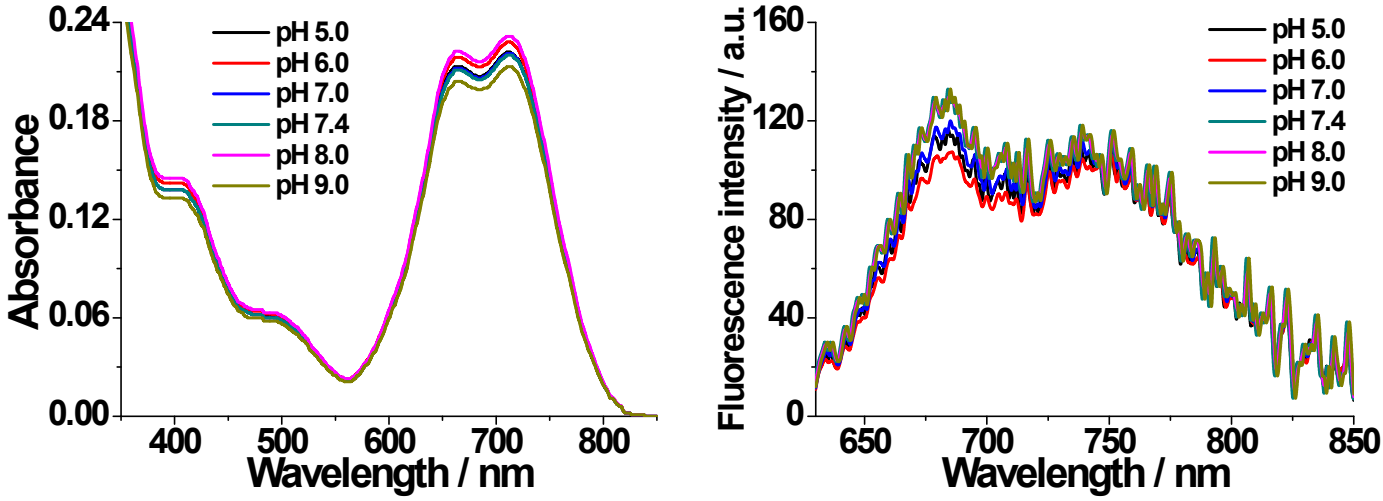

Figure S8. Absorption (left) and fluorescence emission (right) spectra of **PS-Q-NP** (5 μM) in different pH (pH 5 to 9) buffer systems containing 1% DMSO as a cosolvent at 25 °C. The spectra were obtained 12 hours after incubation in each buffer solution. Excited at 600 nm.

4. Properties of PS-A

(a) Fluorescence emission spectra of PS-A as a function of pH: Determination of pK_a of PS-A

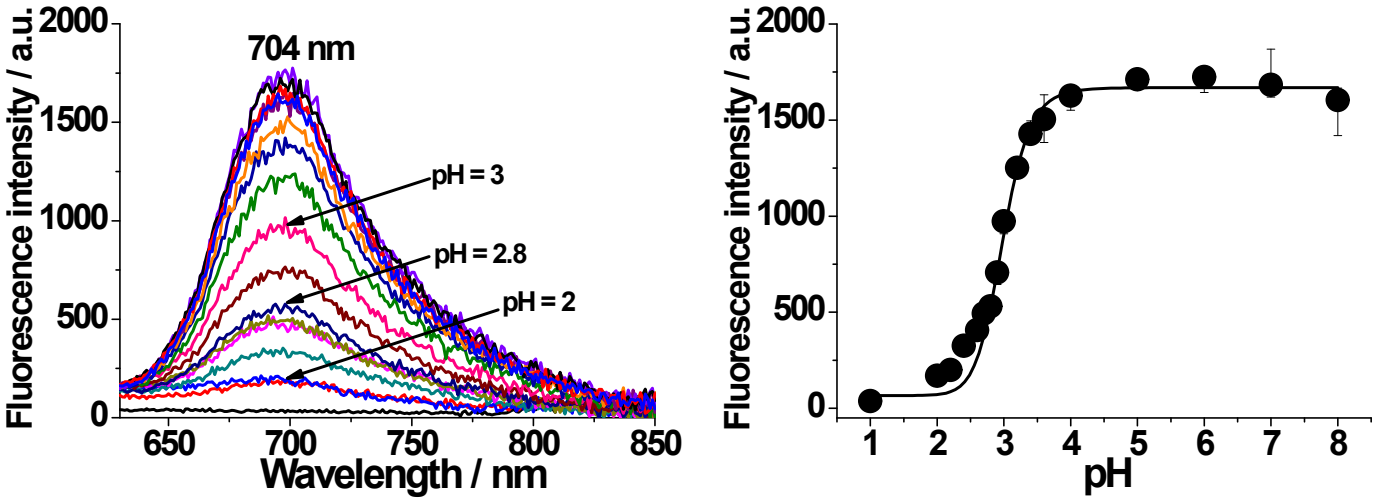

Figure S9. (left) Fluorescence emission spectra and (right) relative fluorescence intensity at 704 nm of **PS-A** in different pH (pH 1 to 8) buffer systems containing 1% DMSO as a cosolvent at 25 °C. [**PS-A**] = 1 μM. Excited at 600 nm. pK_a of **PS-A** is determined to be 2.98.

(b) Stabilities of PS-A in PBS buffer (pH 7.4)

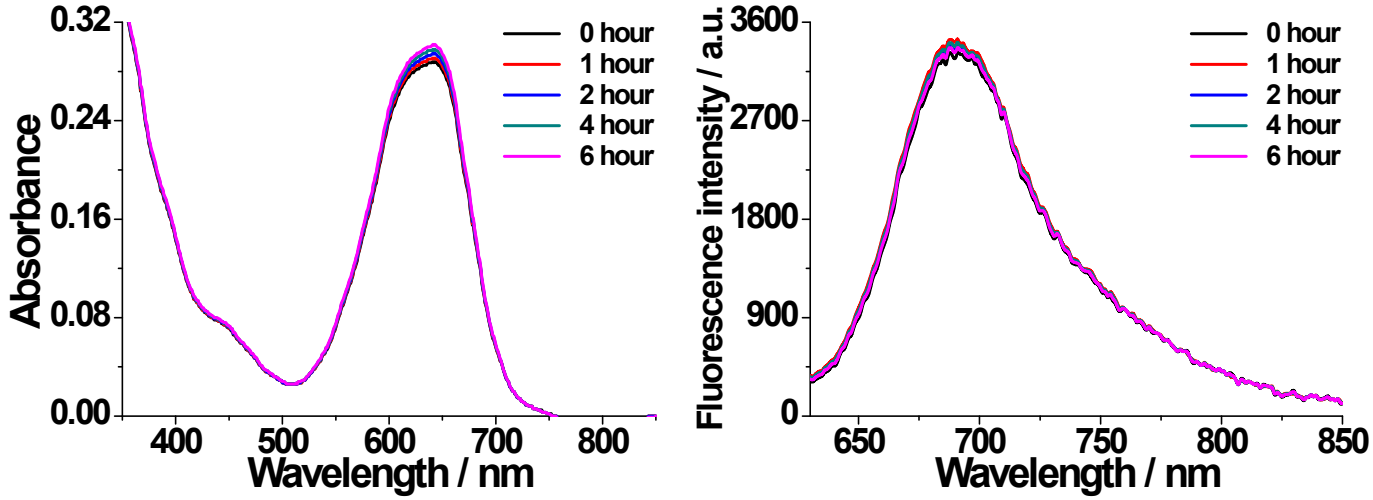

Figure S10. Chemical stability of **PS-A**. Time-dependent absorption (left) and fluorescence emission (λ_{ex} = 600 nm, right) spectra of **PS-A** (5 μM) in PBS (10 mM, pH 7.4, 1% DMSO, 25 °C) under ambient light.

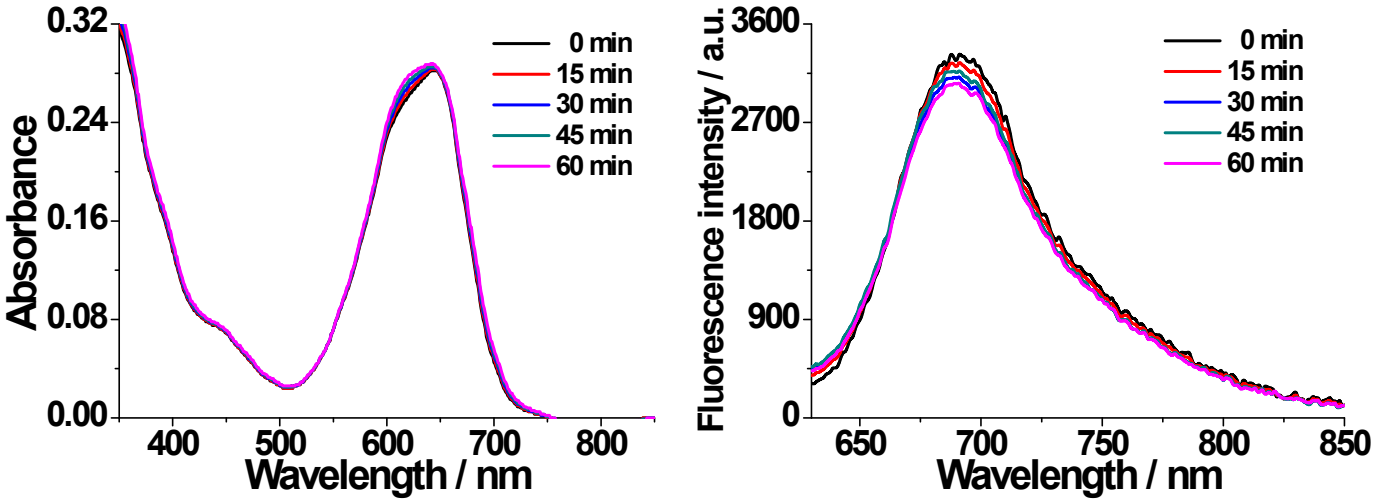

Figure S11. Photostability of **PS-A**. Absorption (left) and fluorescence emission (λ_{ex} = 600 nm, right) spectra of **PS-A** (5 μM) in PBS (10 mM, pH 7.4, 1% DMSO, 25 °C) upon irradiation (670 nm CW laser, 10 mW/cm^2) for indicated time (0–60 min).

5. Evaluation of Singlet Oxygen ($^1O_2$) Generation Efficiency

(a) Determination of $^1O_2$ quantum yields (Φ_Δ) of PS-Q and PS-A in DMSO

A comparative study of $^1O_2$ generation in DMSO was performed by monitoring $^1O_2$-dependent oxidation of 1,3-diphenylisobenzofuran (DPBF)[6] in the presence of the photosensitizer since the absorbance of the DPBF decreases due to the peroxidation of DPBF by the photogenerated $^1O_2$. Each solution containing DPBF (50 μM) and photosensitizer (5 μM) in DMSO was irradiated with a 670 nm CW laser (10 mW/cm^2). The absorbance changes of DPBF at 418 nm were measured every 10 sec for a 3 min period and the decrease of the absorbance caused by photobleaching of DPBF was measured.

The $^1O_2$ quantum yields (Φ_Δ) were calculated according to an established procedure using methylene blue (MB) in DMSO (Φ_Δ = 0.52) as reference.[7] Absorbance of DPBF at 418 nm was plotted against the irradiation time, and the slope was determined for each photosensitizer. The $^1O_2$ quantum yields (Φ_Δ) were estimated by eq. 1:[7]

$$\Phi_\Delta^{PS} = \Phi_\Delta^{Ref} \times \frac{m^{PS}}{m^{Ref}} \times \frac{F^{Ref}}{F^{PS}} \times \frac{PF^{Ref}}{PF^{PS}} \qquad \text{(eq. 1)}$$

where m is the slope of a plot of the change in absorbance of DPBF at 418 nm with the irradiation time, F is the absorption correction factor that can be determined by $F = 1\text{-}10^{-OD}$ (OD = optical density at the irradiation wavelength (670 nm), and PF is an absorbed photonic flux (μ Einstein dm^{-3}s^{-1}). Φ_Δ^{Ref} and Φ_Δ^{PS} are the $^1O_2$ quantum yields for reference (MB) and photosensitizer (**PS-Q** or **PS-A**), respectively,

Table S2. $^1O_2$ quantum yields (Φ_Δ) of compounds in DMSO

Compounds	Φ_Δ[a]
PS-Q conjugate	0.35
PS-A	0.79

[a]Φ_Δ vs methylene blue (Φ_Δ = 0.52 in DMSO).

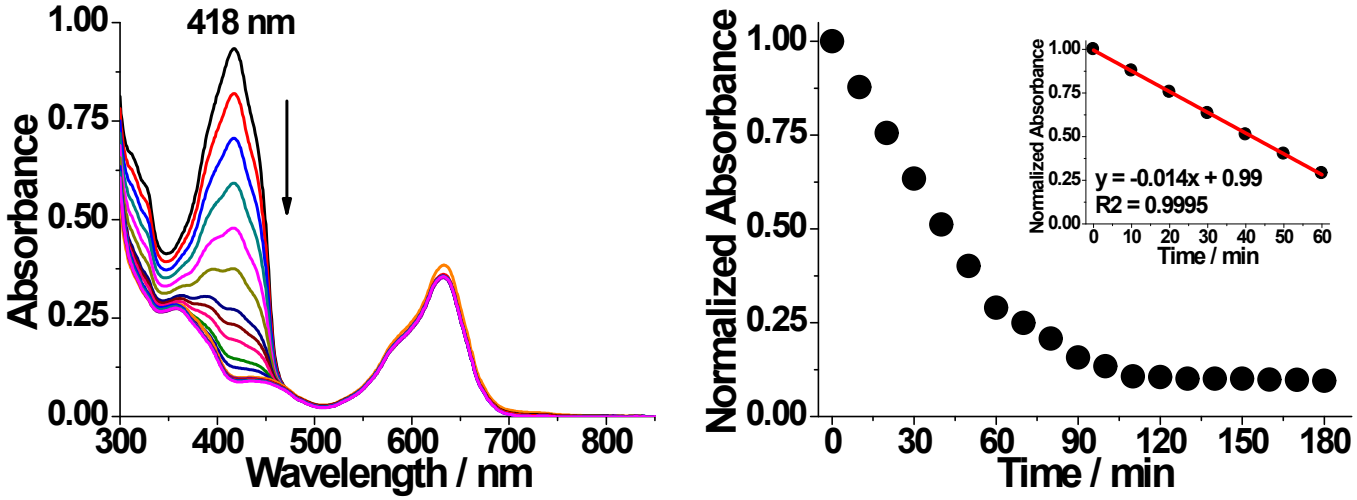

Figure S12. (left) Absorption spectra of DPBF (50 μM) in the presence of **PS-A** (5 μM) in DMSO upon irradiation (670 nm laser, 10 mW/cm^2) for 180 sec (top to bottom: 0 to 180 sec, interval = 10 sec). (right) Plot of change in absorbance at 418 nm of DPBF as a function of irradiation time in the presence of **PS-A** in DMSO. Inset: Linear relationships between the normalized absorbance at 418 nm and irradiation time (0–60 sec) in the presence of **PS-A** in DMSO.

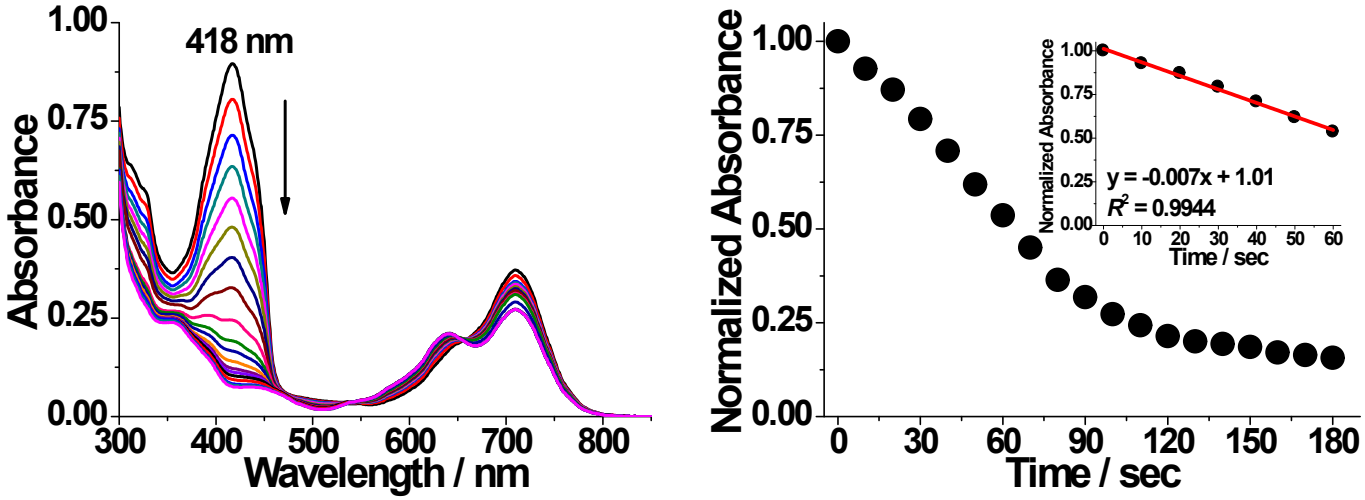

Figure S13. (left) Absorption spectra of DPBF (50 μM) in the presence of **PS-Q** conjugate (5 μM) in DMSO upon irradiation (670 nm laser, 10 mW/cm^2) for 180 sec (top to bottom: 0 to 180 sec, interval = 10 sec). (right) Plot of change in absorbance of DPBF at 418 nm as a function of irradiation time in the presence of **PS-Q** conjugate in DMSO. Inset: Linear relationships between the normalized absorbance at 418 nm and irradiation time (0–60 sec) in the presence of **PS-Q** conjugate in DMSO.

(b) Determination of $^1O_2$ quantum yields (Φ_Δ) of PS-Q and PS-A in PBS buffer

The $^1O_2$ generation in an aqueous buffer solution was measured using singlet oxygen sensor green® (SOSG),[8] as an indicator. In the presence of $^1O_2$, SOSG emits strong green fluorescence ($\lambda_{ex,\,max}/\lambda_{em,\,max}$ = 460/528 nm), which corresponds to the formation of an endoperoxide by the reaction of $^1O_2$ with the anthracene component of SOSG. Each solution containing SOSG (1 μM) and photosensitizer (5 μM) in PBS buffer (10 mM, pH 7.4, 1% DMSO) was irradiated with a 670 nm CW laser (10 mW/cm^2). Increase in the fluorescence intensity at 528 nm was measured every 30 sec for 8 min.

The $^1O_2$ quantum yields (Φ_Δ) were calculated according to a reported procedure using methylene blue (MB) in PBS buffer (Φ_Δ = 0.39) as reference.[9] The fluorescence intensity at 528 nm was plotted against the irradiation time and the slope was determined for each photosensitizer. The $^1O_2$ quantum yields (Φ_Δ) were estimated by eq. 2:

$$\Phi_\Delta^{PS} = \Phi_\Delta^{Ref} \times \frac{k^{PS}}{k^{Ref}} \times \frac{I^{Ref}}{I^{PS}} \qquad \text{(eq. 2)}$$

where Φ_Δ^{Ref} and Φ_Δ^{PS} are the $^1O_2$ quantum yields for reference (MB) and photosensitizer (**PS-Q** or **PS-A**), respectively, and k^{Ref} and k^{PS} are the first order reaction rate constants of SOSG with reference (MB) and photosensitizer (**PS-Q** or **PS-A**), respectively. I^{Ref} and I^{PS} represent light absorbed by MB and photosensitizer at irradiation wavelength (670 nm), respectively.

Table S3. $^1O_2$ quantum yields (Φ_Δ) of compounds in PBS (10 mM, pH 7.4, 1% DMSO)

Compounds	Φ_Δ[a]
PS-Q-NP alone	0.003
PS-Q-NP + GSH (0.01 mM)	0.0037
PS-Q-NP + GSH (0.10 mM)	0.03
PS-Q-NP + GSH (1.00 mM)	0.12
PS-A alone	0.15

[a] $^1O_2$ quantum yields (Φ_Δ) vs methylene blue (Φ_Δ = 0.39 in PBS).

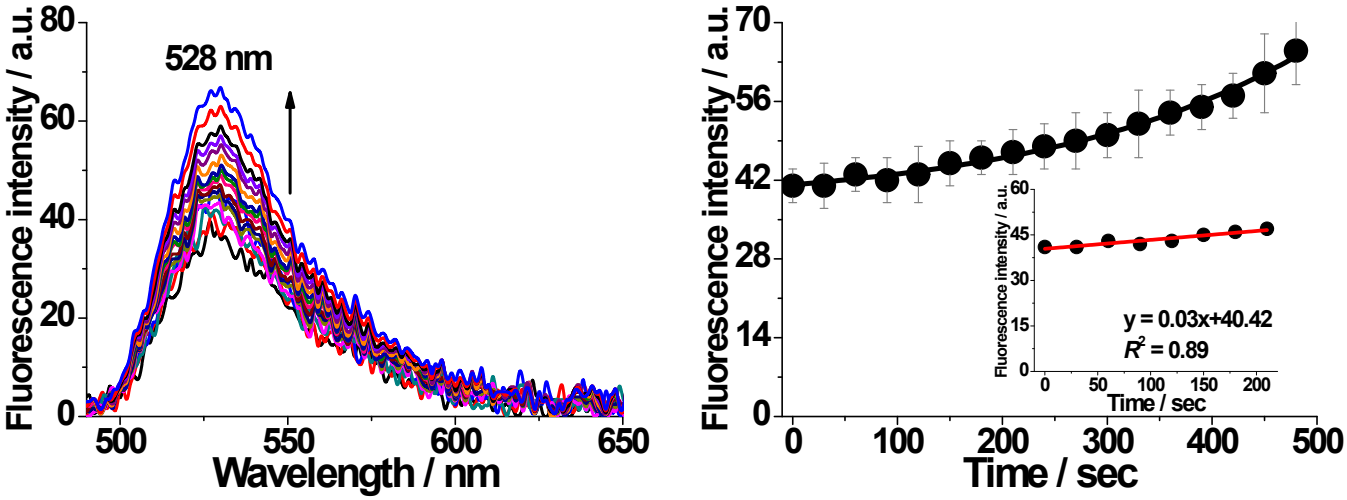

Figure S14. (left) Fluorescence spectra of SOSG (1 μM) in the presence of **PS-Q-NP** (5 μM) in PBS (10 mM, pH 7.4, 1% DMSO, 25 °C) upon irradiation (670 nm laser, 10 mW/cm^2) for 8 min (bottom to top: 0 to 8 min, interval = 30 sec). Excited at 460 nm. (right) Plot of change in fluorescence intensity at 528 nm of SOSG as a function of irradiation time in the presence of **PS-Q-NP** in PBS buffer. Inset: Linear relationships between the emission at 528 nm and irradiation time (0–200 sec) in the presence of **PS-Q-NP**.

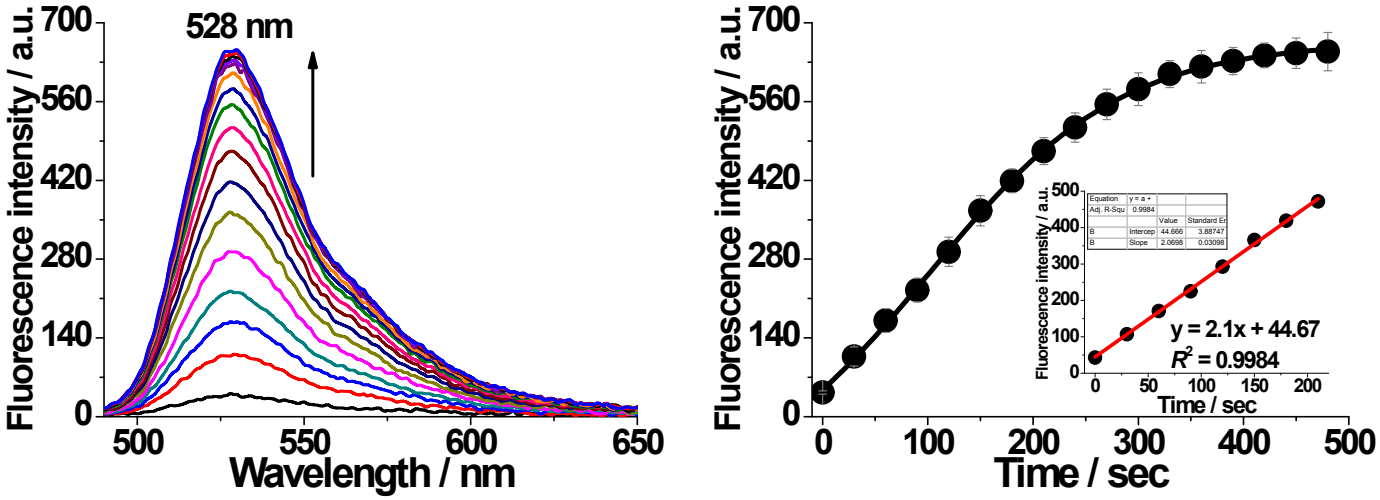

Figure S15. (left) Fluorescence spectra of SOSG (1 μM) in the presence of **PS-A** (5 μM) in PBS (10 mM, pH 7.4, 1% DMSO, 25 °C) upon irradiation (670 nm laser, 10 mW/cm^2) for 8 min (bottom to top: 0 to 8 min, interval = 30 sec). Excited at 460 nm. (right) Plot of change in fluorescence intensity at 528 nm of SOSG as a function of irradiation time in the presence of **PS-A** in PBS buffer. Inset: Linear relationships between the emission at 528 nm and irradiation time (0–200 sec) in the presence of **PS-A**.

(c) $^1O_2$ generation of PS-Q in the presence of GSH (0.01, 0.1, and 1 mM)

We also investigated the effect of GSH on $^1O_2$ generation of **PS-Q-NP** in PBS (10 mM, pH 7.4, 1% DMSO) at 25 °C. **PS-Q-NP** (5 μM, 196 μL) was incubated with GSH at different concentrations (0.01, 0.1, and 1 mM, 2 μL) for 5 min, and then SOSG in MeOH (2 μL) was added to each assay solution. After each solution was irradiated with a 670 CW laser (10 mW/cm^2) for the indicated time periods, fluorescence emission spectra for each solution was recorded using a computer-controlled fluorescence plate reader.

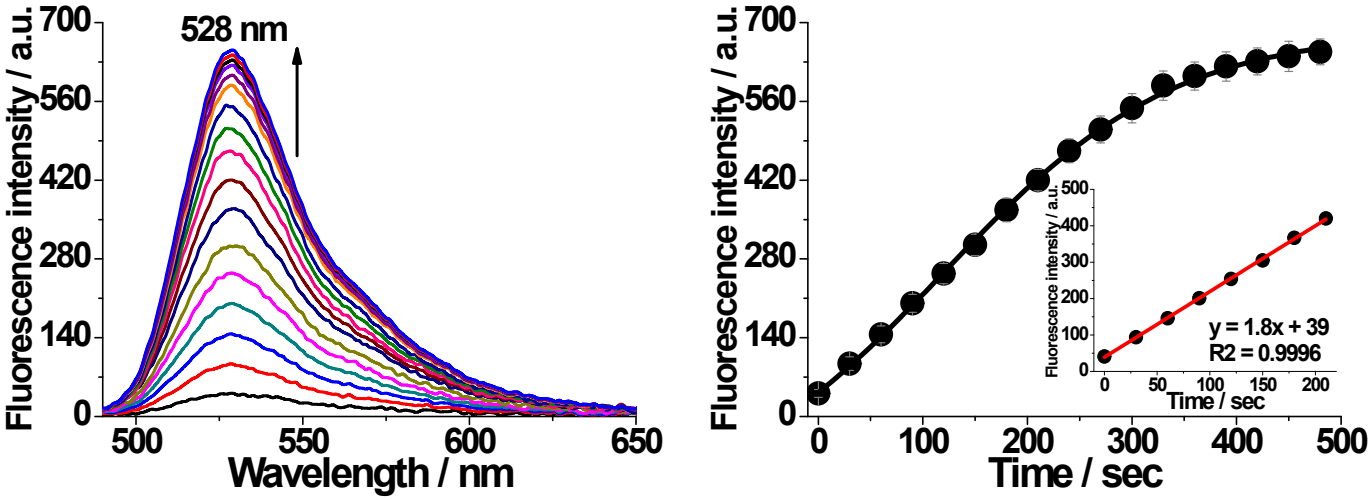

Figure S16. $^1O_2$ generation of **PS-Q-NP** in the presence of GSH (1 mM). (left) Fluorescence spectra of SOSG (1 μM) in the presence of **PS-Q-NP** (5 μM) upon irradiation (670 nm CW laser, 10 mW/cm^2) for 8 min (bottom to top: 0 to 8 min, interval = 30 sec). **PS-Q-NP** was pre-incubated with GSH (1 mM) for 5 min before laser irradiation. Excited at 460 nm. (right) Plot of change in fluorescence intensity at 528 nm of SOSG as a function of irradiation time in the presence of **PS-Q-NP** pretreated with GSH (1 mM). Inset: Linear relationships between the emission at 528 nm and irradiation time (0–200 sec) in the presence of **PS-Q-NP** pretreated with GSH (1 mM). All data were obtained in PBS (10 mM, pH 7.4, 1% DMSO) at 25 °C.

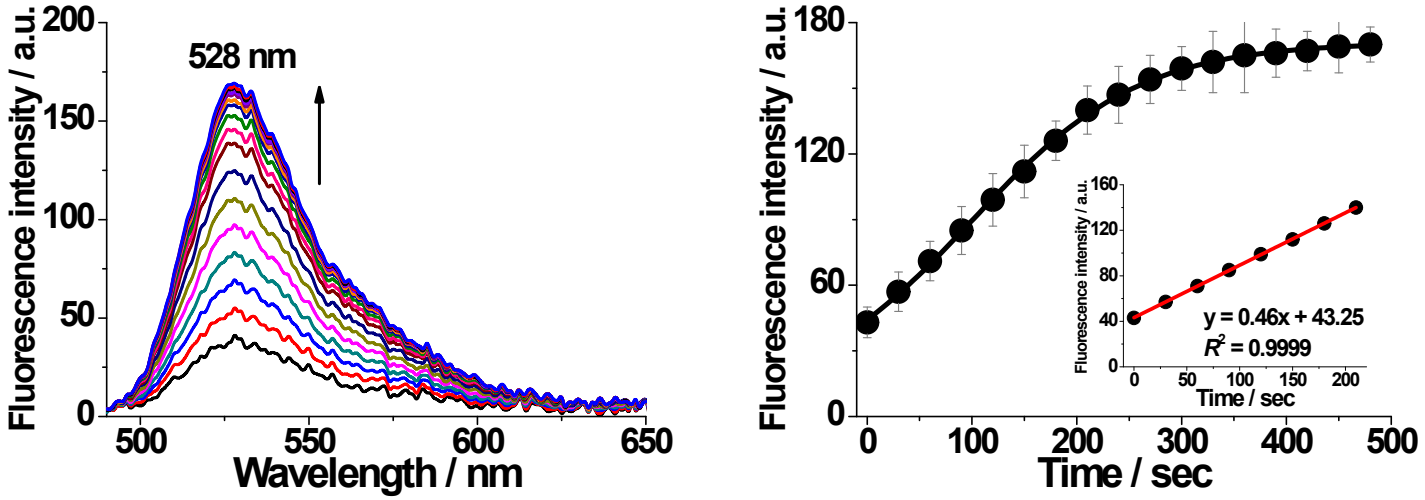

Figure S17. $^1O_2$ generation of **PS-Q-NP** in the presence of GSH (0.1 mM). (left) Fluorescence spectra of SOSG (1 μM) in the presence of **PS-Q-NP** (5 μM) upon irradiation (670 nm CW laser, 10 mW/cm^2) for 8 min (bottom to top: 0 to 8 min, interval = 30 sec). **PS-Q-NP** was pre-incubated with GSH (0.1 mM) for 5 min before laser irradiation. Excited at 460 nm. (right) Plot of change in fluorescence intensity at 528 nm of SOSG as a function of irradiation time in the presence of **PS-Q-NP** pretreated with GSH (0.1 mM). Inset: Linear relationships between the emission at 528 nm and irradiation time (0–200 sec) in the presence of **PS-Q-NP** pretreated with GSH (0.1 mM). All data were obtained in PBS (10 mM, pH 7.4, 1% DMSO) at 25 °C.

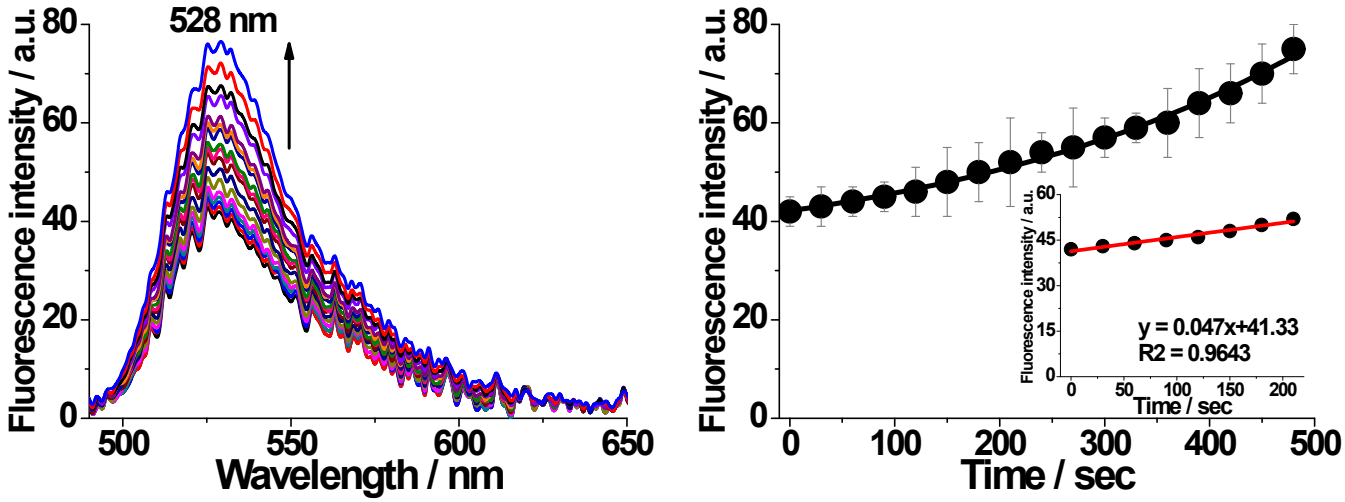

Figure S18. $^1O_2$ generation of **PS-Q-NP** in the presence of GSH (0.01 mM). (left) Fluorescence spectra of SOSG (1 μM) in the presence of **PS-Q-NP** (5 μM) upon irradiation (670 nm CW laser, 10 mW/cm^2) for 8 min (bottom to top: 0 to 8 min, interval = 30 sec). **PS-Q-NP** was pre-incubated with GSH (0.01 mM) for 5 min before laser irradiation. Excited at 460 nm. (right) Plot of change in fluorescence intensity at 528 nm of SOSG as a function of irradiation time in the presence of **PS-Q-NP** pretreated with GSH (0.01 mM). Inset: Linear relationships between the emission at 528 nm and irradiation time (0–200 sec) in the presence of **PS-Q-NP** pretreated with GSH (0.01 mM). All data were obtained in PBS (10 mM, pH 7.4, 1% DMSO) at 25 °C.

6. GSH-Induced Fluorescence Activation of PS-Q-NP

Glutathione (GSH, reduced form) was dissolved in water to give final concentrations ranging from 0–5000 μM. An amount of 2 μL of **PS-Q** conjugate (final concentration = 5 μM) dissolved in DMSO was added to 196 μL of PBS (10 mM, pH 7.4), followed by the addition of 2 μL of GSH solution. This solution was incubated at 25 °C for the indicated time periods. Fluorescence intensity at 691 nm was recorded using a computer-controlled fluorescence plate reader.

(a) Absorption and fluorescence emission responses of PS-Q-NP upon incubation with GSH (0.5 mM)

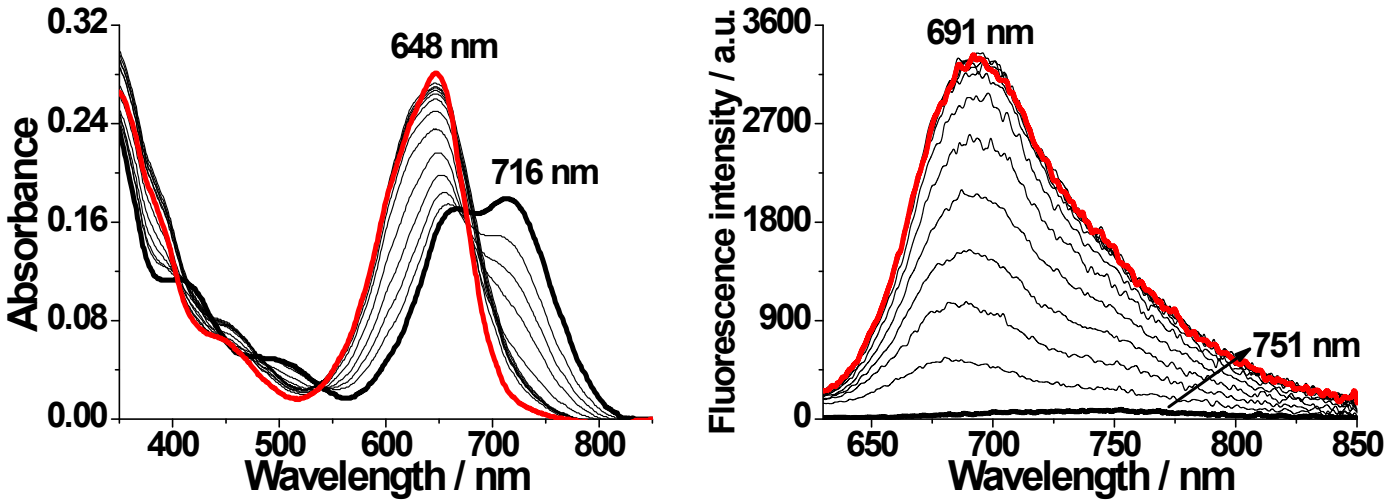

Figure S19. Time-dependent absorption (left) and fluorescence emission (right) spectra of **PS-Q-NP** (5 μM) upon treatment with GSH (0.5 mM) in PBS (10 mM, pH 7.4, 1% DMSO) at 25 °C. The spectra were obtained every 30 sec (0–6 min) after addition of GSH to **PS-Q-NP**. Excited at 600 nm. The black and red lines indicate spectra of **PS-Q-NP** before and 6 min after addition of GSH, respectively.

(b) Fluorescence activation of PS-Q-NP upon incubation with different amounts of GSH (0–5 mM)

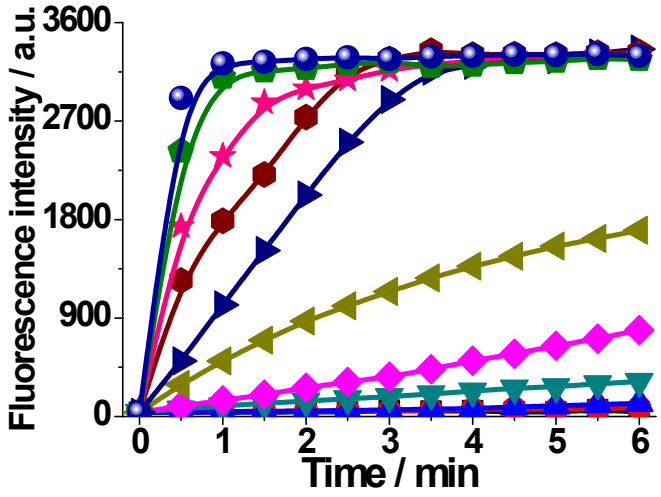

Figure S20. Time-dependent monitoring of fluorescence intensity at 691 nm upon incubation of **PS-Q-NP** (5 μM) with different amounts of GSH (bottom to top: 0, 0.005, 0.01, 0.05, 0.1, 0.25, 0.5, 0.75, 1, 2.5, 5 mM). The emission spectra were obtained every 30 sec (0–6 min) after the addition of GSH to **PS-Q-NP** in PBS (10 mM, pH 7.4, 1% DMSO) at 25 °C. Excited at 600 nm.

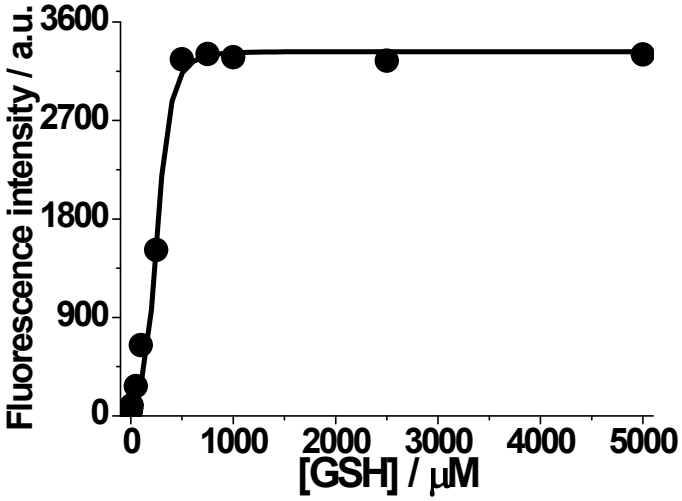

Figure S21. Relative fluorescence intensity at 691 nm of **PS-Q-NP** (5 μM) upon treatment with GSH at different concentrations (0, 0.005, 0.01, 0.05, 0.1, 0.25, 0.5, 0.75, 1, 2.5, 5 mM). All data were obtained 5 min after the addition of GSH to **PS-Q-NP** in PBS (10 mM, pH 7.4, 1% DMSO) at 25 °C. Excited at 600 nm.

(c) Control experiment: absorption and fluorescence emission responses of PS-E toward GSH (1 mM)

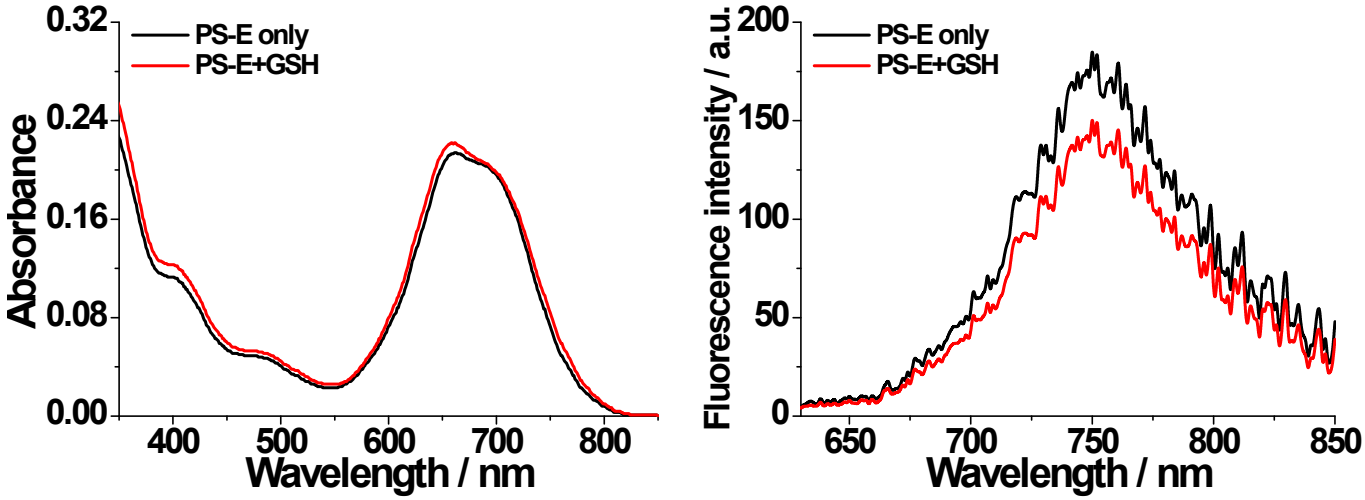

Figure S22. Absorption (left) and fluorescence emission (right) spectra of **PS-E** (5 μM) upon treatment with GSH (1 mM) in PBS (10 mM, pH 7.4, 1% DMSO, 25 °C) for 1 h. Excited at 600 nm. The black and red lines indicate spectra of **PS-E** before and 1 h after addition of GSH, respectively.

(d) Control experiment: absorption and fluorescence emission responses of PS-A toward GSH (1 mM)

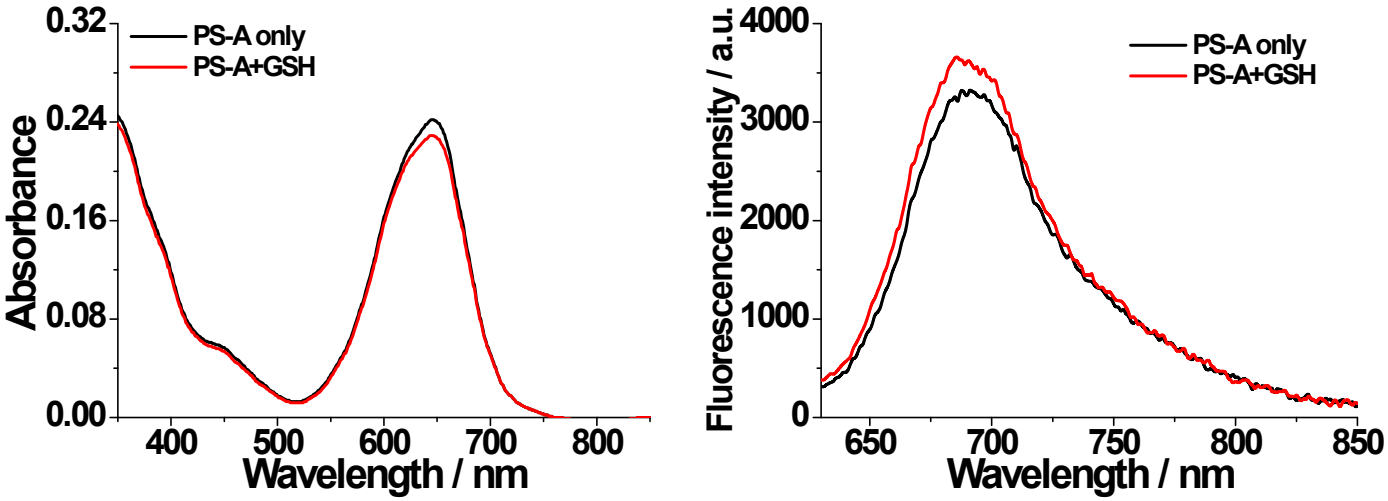

Figure S23. Absorption (left) and fluorescence emission (right) spectra of **PS-A** (5 μM) upon treatment with GSH (1 mM) in PBS (10 mM, pH 7.4, 1% DMSO, 25 °C) for 1 h. Excited at 600 nm. The black and red lines indicate spectra of **PS-A** before and 1 h after addition of GSH, respectively.

(e) Selective fluorescence activation of PS-Q-NP by biological reductants

*Fluorescence response of **PS-Q-NP** toward various biological species*

Various reactive oxygen species (ROSs) were prepared as follows: Superoxide ($\cdot O_2^-$) was added as solid KO_2. Hydrogen peroxide (H_2O_2), *tert*-butyl hydroperoxide (TBHP), and sodium hypochlorite (NaOCl) were delivered from 30%, 70%, and 5% aqueous solutions, respectively. Hydroxyl radical ($\cdot$OH) was generated by Fenton reaction of Fe^{2+} with H_2O_2.

***Note.** The intracellular concentrations of homocysteine ([Hcy] = ca. 10 μM) and cysteine ([Cys] = ca. 30–200 μM) are significantly lower than with that of GSH (1–10 mM). However, fluorescence responses of **PS-Q-NP** were studied with the same amounts (1 mM) of Hcy, Cys and GSH (Figure S24).*

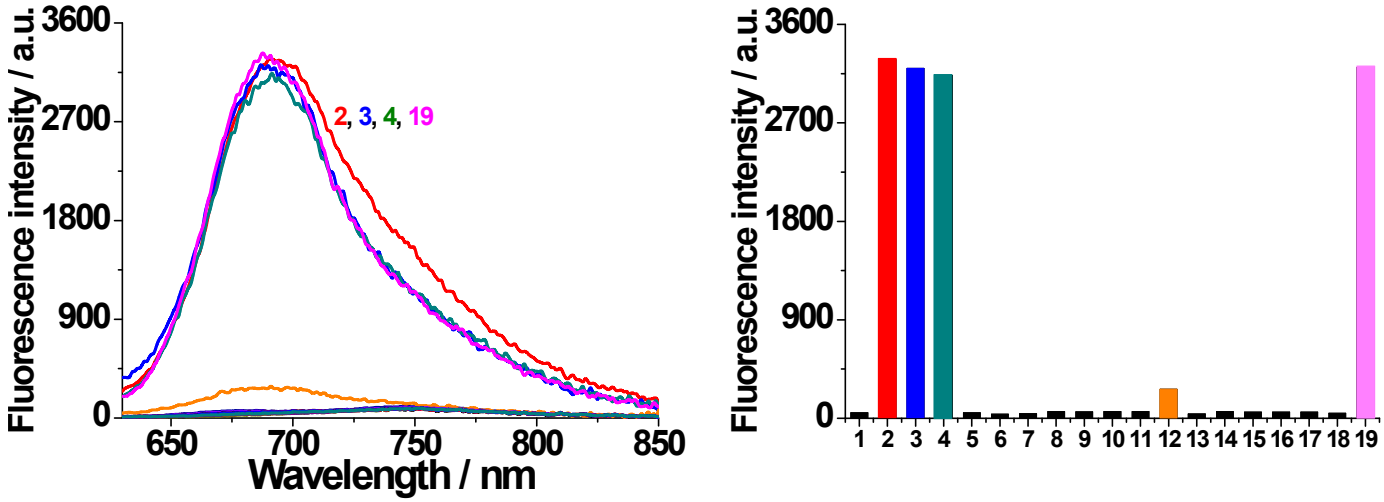

Figure S24. (left) Fluorescence emission spectra and (right) relative fluorescence intensity at 691 nm of **PS-Q-NP** (5 μM) upon treatment with various biological species: (1) Control: **PS-Q-NP** only, (2) reduced glutathione (GSH), (3) cysteine, (4) homocysteine, (5) oxidized glutathione (GSSG), (6) esterase, (7) lipase, (8) trypsin, (9) lysine, (10) serine, (11) glucose, (12) BSA, (13) H_2O_2, (14) NaOCl, (15) $\cdot$OH, (16) $\cdot O_2^-$, (17) TBHP, (18) NADH, (19) hNQO1+NADH. All data were obtained 5 min after the addition of each analyte to **PS-Q-NP** in PBS (10 mM, pH 7.4, 1% DMSO) at 25 °C. Excited at 600 nm. [esterase] = 1 U/mL, [lipase] = [trypsin] = 1 mg/mL, [BSA] = 5 μM. [NQO1] = 5 μg/mL, [Others] = 1 mM.

*Stability of **PS-Q-NP** itself toward light irradiation.*

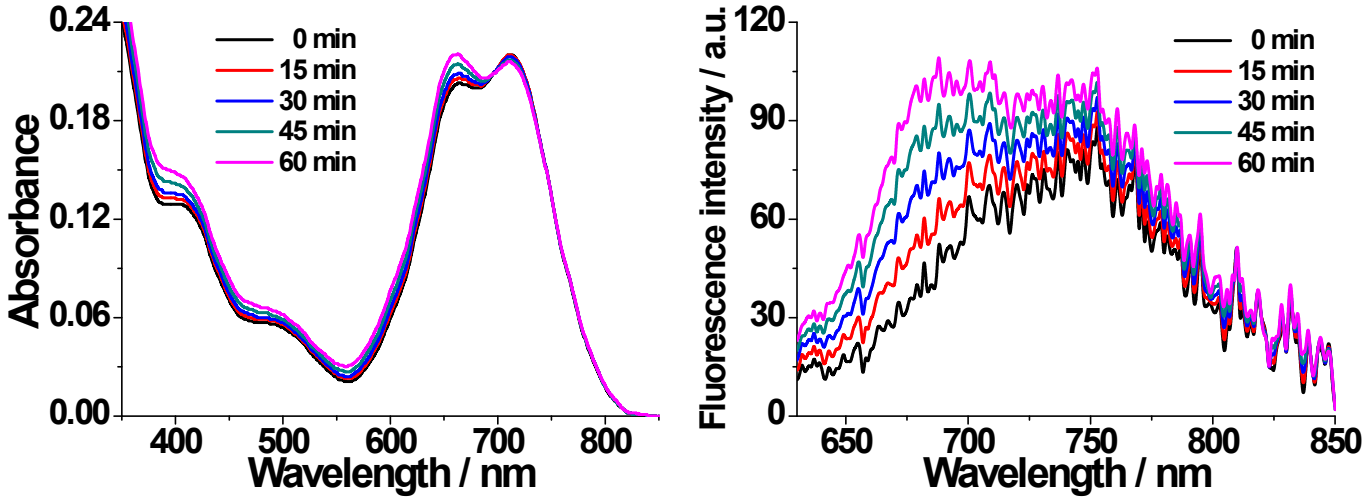

Figure S25. Time-dependent absorption (left) and fluorescence emission (right) spectra of **PS-Q-NP** (5 μM) in PBS (10 mM, pH 7.4, 1% DMSO) upon irradiation (670 nm laser, 10 mW/cm^2) for 60 min at 25 °C. Excited at 600 nm.

7. Two Plausible Mechanisms for "Turn-on" Fluorescence and Photosensitizing Activities

(a) Conversion of PS-Q-NP to PS-A: the Michael addition of thiols to quinone, followed by quinone-methide-type rearrangement

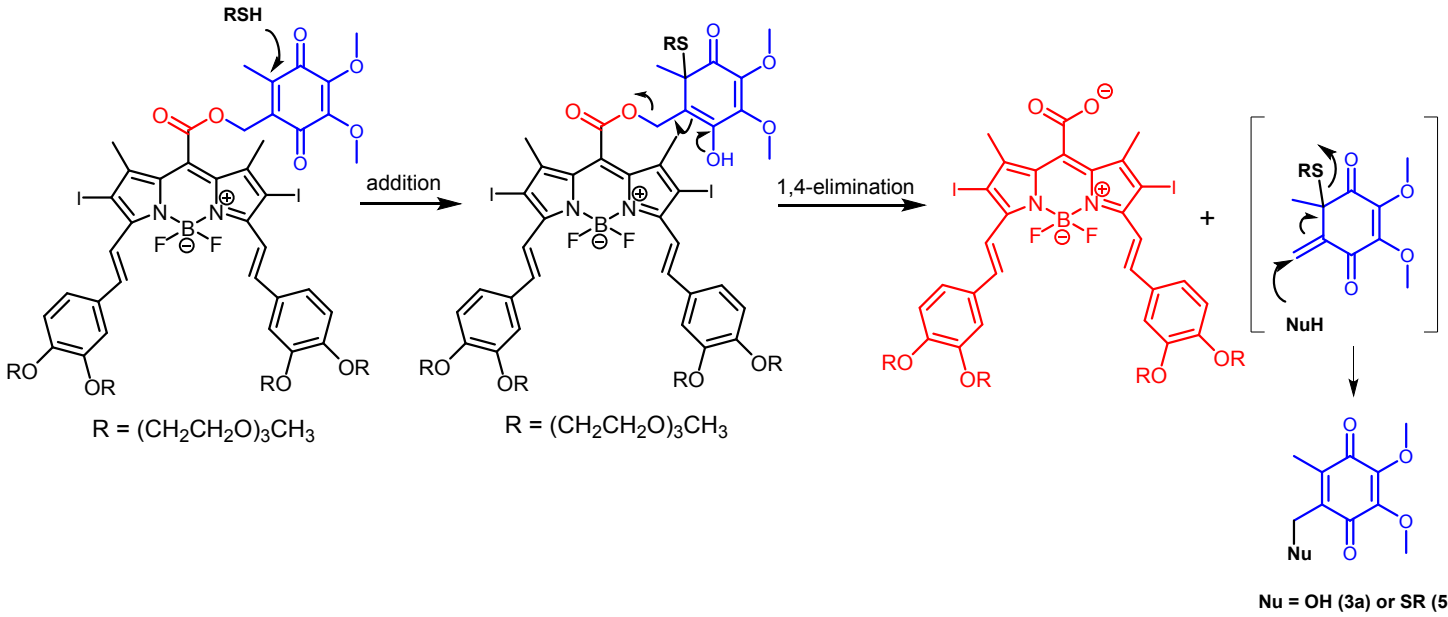

Nu = OH (3a) or SR (5a)

(b) Conversion of PS-Q-NP to PS-A: the reduction of quinone by thiols, followed by quinone-methide-type rearrangement

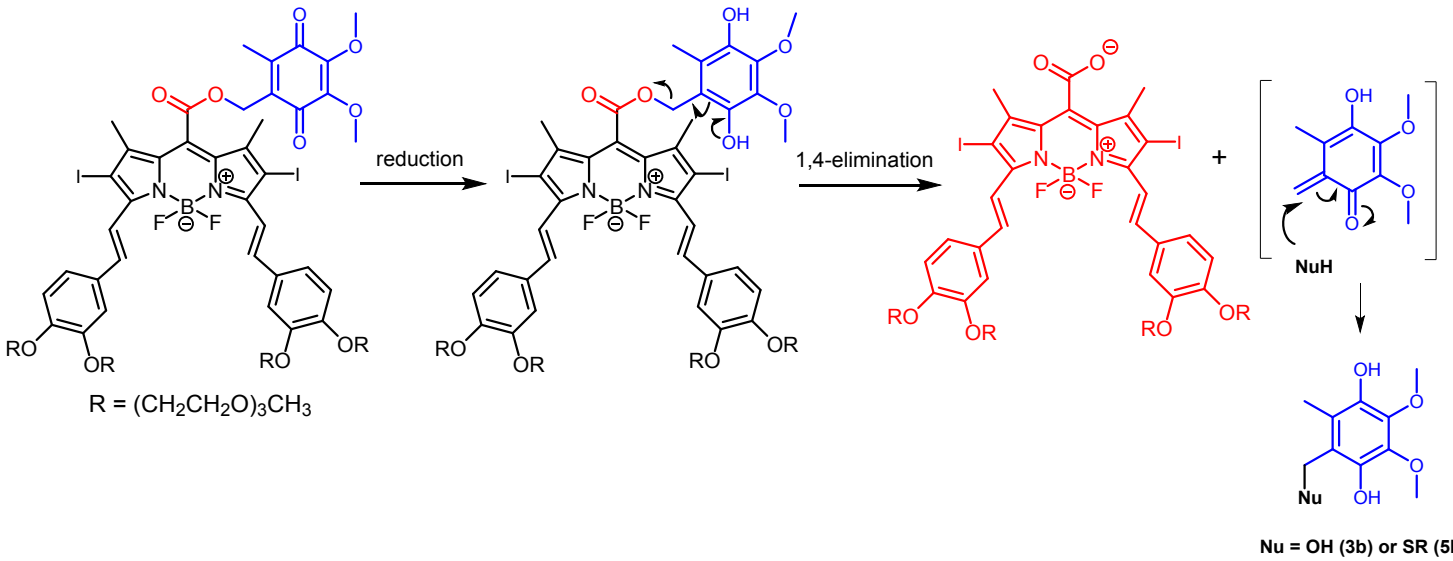

Nu = OH (3b) or SR (5b)

8. Confirmation of PS-Q-NP to PS-A Conversion by LC-MS Analysis

(a)

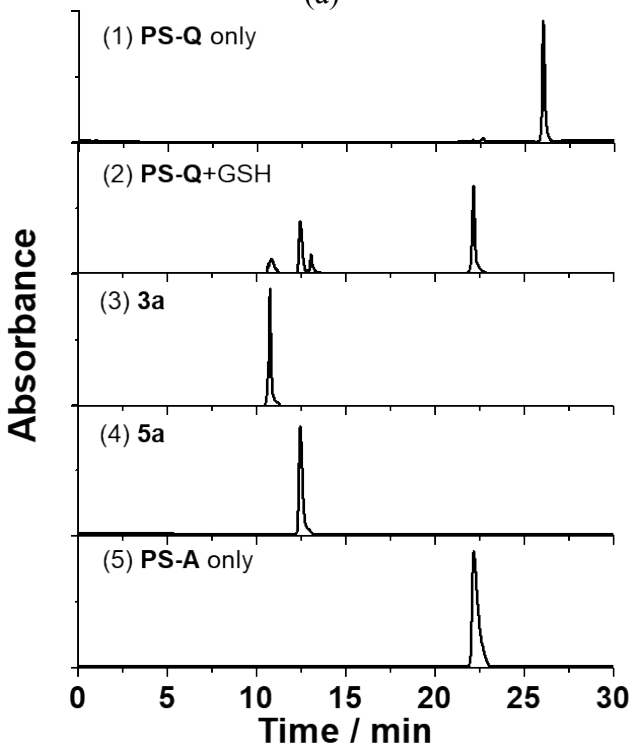

(b) Retention time = 10.8 min

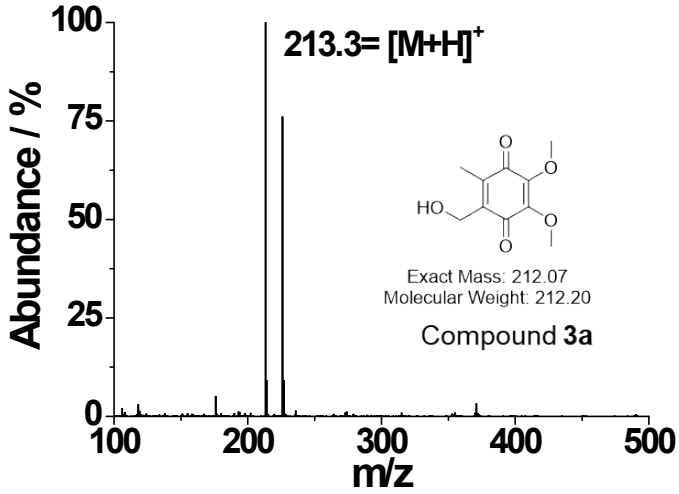

(c) Retention time = 11.0 min

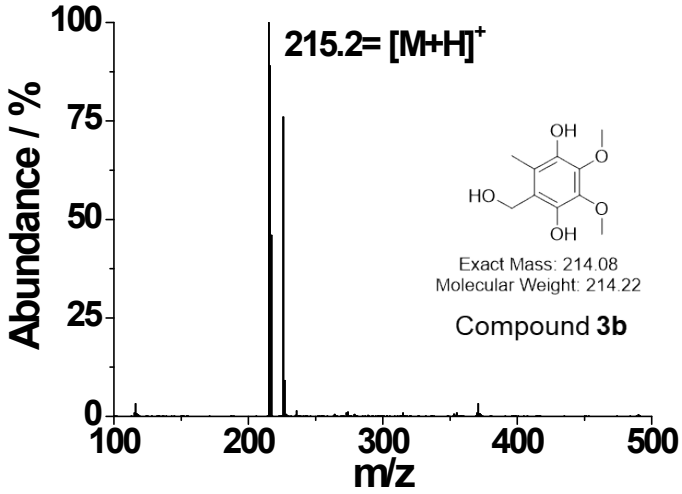

(d) Retention time = 12.4 min

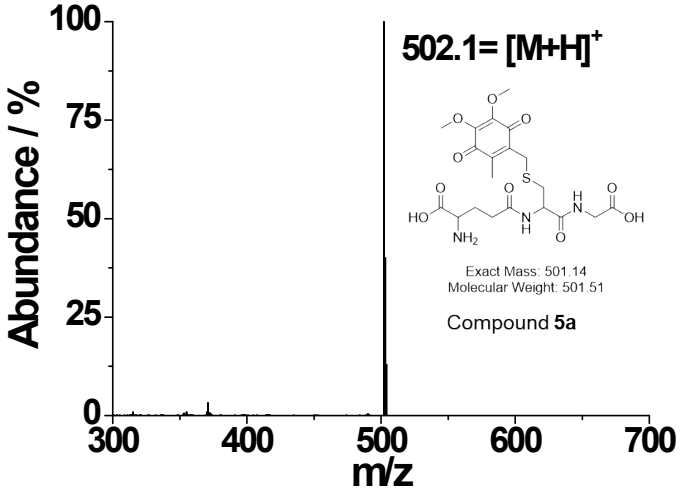

(e) Retention time = 13.0 min

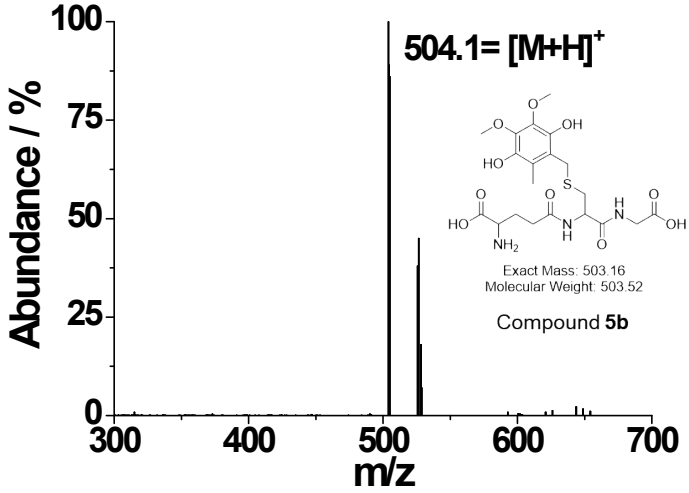

(f) Retention time = 22.3 min

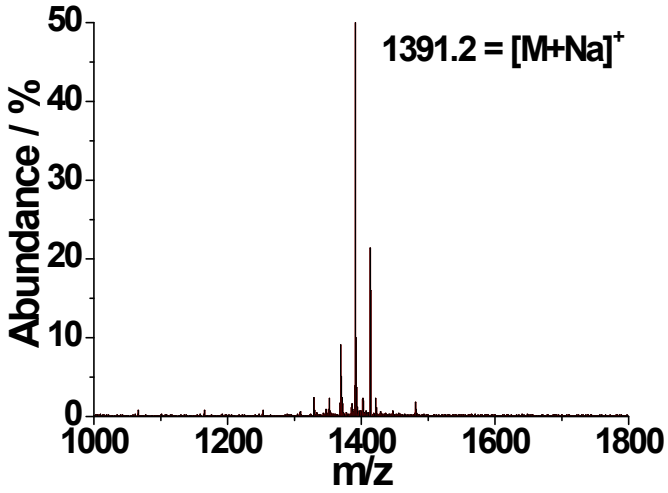

(g) Retention time = 26.7 min

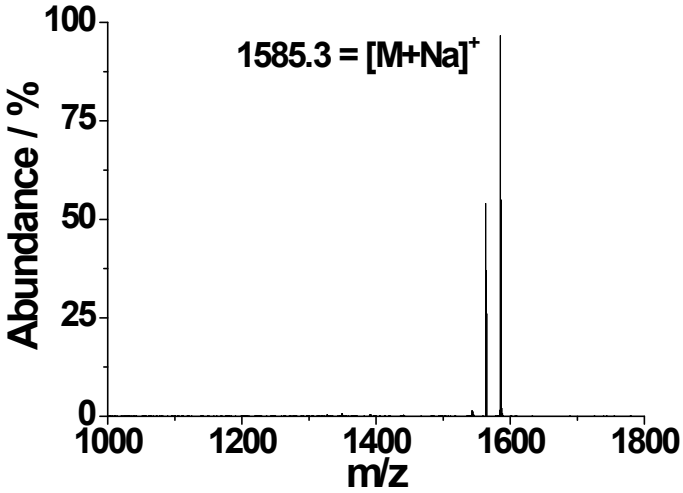

Figure S26. (a) HPLC chromatograms of **PS-Q** conjugate (20 μM) before (1) and after (2) treatment with GSH (5 mM) for 5 min at 25 °C; **3a** (3); **5a** (4); **PS-A** only (5). The samples were analyzed by LC-MS with a linear gradient elution (from 30 to 100% A, A: MeOH with 5 mM ammonium formate, B: deionized water with 0.1% formic acid, degassing with nitrogen for 30 min, flow rate 0.3 mL/min, UV-Vis: 250±20 nm and 540 nm). ESI-MS spectra of the peak of retention time at (b) 10.8 min, (c) 11.0 min, (d) 12.4 min, (e) 13.0 min, (f) 22.3 min, and (g) 26.7 min. MW of the retention time at 10.8 min is 213.3, which corresponds to $[M+H]^+$ for compound **3a**, MW of the retention time at 11.0 min is 215.2, which corresponds to $[M+H]^+$ for compound **3b**, MW of the retention time at 12.4 min is 502.1, which corresponds to $[M+H]^+$ for compound **5a**, MW of the retention time at 13.0 min is 504.1, which corresponds to $[M+H]^+$ for compound **5b**, MW of the retention time at 22.3 min is 1391.2, which corresponds to $[M+Na]^+$ for **PS-A**, MW of the retention time at 26.7 min is 1585.3, which corresponds to $[M+Na]^+$ for **PS-Q** conjugate. [**3a**] = [**5a**] = [**PS-A**] = 20 μM.

9. Cell Studies

(a) Cell culture

U87-MG cell line (human glioblastoma) was obtained from American Type Culture Collection (ATCC, Rockville, MD, USA), and cultured in Dulbecco's Modified Eagle's Medium (DMEM) supplemented with 10% (v/v) fetal bovine serum (FBS), 1% antibiotic-antimycotic in a humidified incubator containing 5% CO_2 at 37 °C.

(b) Confocal fluorescence microscopy

U87-MG cells were seeded at a density of 1×10^5 cells/well in a 4-well Lab Tek-II chambered cover glass (Nalge Nunc International Corp., Rochester) and incubated for 24 hours for cell attachment. Cells were treated with photosensitizer (**PS-A** and **PS-Q-NP**) for 4 hours at 5 μM concentration. After washing, the cells were incubated with LysoTracker (100 nM, Blue DND-22, Thermo Scientific) for 30 minutes to stain the lysosomes of the cancer cells. Next, the cells were washed 3 times with cell culture medium, and then fluorescence images of the photosensitizer (λ_{ex} = 633 nm, λ_{em} = 638–755 nm) and LysoTracker (λ_{ex} = 405 nm, λ_{em} = 410-488 nm) in the cells were obtained using confocal laser scanning microscopy (Carl Zeiss LSM 880 Plan-Apochromat 20x/0.80 M27, Germany). Co-localization in the fluorescence signals of the photosensitizers with LysoTracker was analyzed using Zen software (Blue edition, Carl Zeiss, Germany).

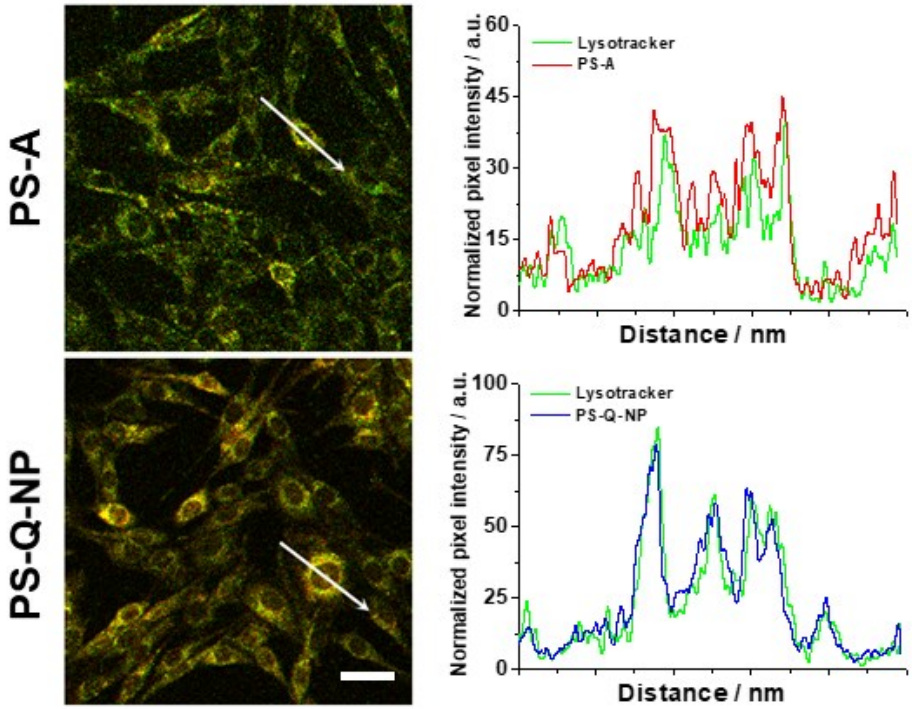

Figure S27. Co-localization of photosensitizer (top: **PS-A**; bottom: **PS-Q-NP**) with Lysotracker in U87-MG cells. Fluorescence intensities of the photosensitizer and Lysotracker in the white arrow region were analyzed using Zen software and compared. Red and green colored lines indicates fluorescence intensities of the photosensitizer (top: **PS-A**; bottom: **PS-Q-NP**) and Lysotracker, respectively. Scale bar = 20 μm.

(c) In vitro phototoxicity and cytotoxicity tests

U87-MG cells were seeded at a density of 1×10^4 cells/well in a 96-well plate (Nunc, ThermoFisher, MA, USA) and incubated for 24 h for cell attachment. The cells were treated with photosensitizer (**PS-A** and **PS-Q-NP**) for 4 h at various concentrations (0, 0.625, 1.25, 2.5, 5, and 10 μM). After washing the cells 3 times with cell culture medium, the cells were irradiated with a 670 CW laser at a light dose rate of 50 mW/cm^2 for 200 sec (light dose: 10 J/cm^2), and then further incubated for 18 h. Then, cell viability (n = 4) was analyzed using a CCK-8 assay kit (Dojindo Laboratories, Mashikimachi, Kumamoto, Japan). LD_{50} of **PS-Q-NP** is determined to be 3.24 μM. Untreated control cells were used as a reference for 100% viable cells, while the cell culture medium served as the background. For cytotoxicity test, the cells were treated with photosensitizer (**PS-A** and **PS-Q-NP**) for 4 h at the same concentrations described above. After washing the cells 3 times with cell culture medium, the cells were incubated for 18 h without light irradiation. Then, cell viability (n = 4) was analyzed using a CCK-8 assay kit.

(d) Effect of GSH inhibition

L-Buthionine sulfoximine (BSO, Merck KGaA, Germany), a specific inhibitor of glutathione (GSH) synthesis, was used to inhibit conversion of **PS-Q-NP** to **PS-A** by GSH. U87-MG cells were seeded at a density of 1×10^5 cells/well in a 4-well Lab Tek-II chambered cover glass and incubated for 24 h for cell attachment. The cells were pre-treated with 0.4 mM BSO for 24 h to inhibit GSH synthesis,[10] washed, and then treated with **PS-Q-NP** for 4 h at the concentration of 5 μM. Then, the cells were washed 3 times with cell culture medium. Confocal fluorescence images of the cells (λ_{ex} = 633 nm, λ_{em} = 638-755 nm) were obtained using confocal laser scanning microscope (Carl Zeiss LSM 780 Plan-Apochromat 40x/1.2 W Korr FCS M27, Germany). For comparison, fluorescence image of the cells without pretreatment of BSO was also checked.

10. *In vivo* studies

In vivo fluorescence imaging

Activation of optical property of **PS-Q-NP** by GSH was evaluated in the tumor xenograft model. All animal studies were approved by the Institutional Animal Care and Use Committee. 5 Weeks olds female athymic Balb/c nude mice were used for *in vivo* imaging. U87-MG (5 x 10^6 cells/100 μL) were subcutaneously implanted into the right flanks of mice. A total of 9 mice were used for imaging study, and their tumor size reached ~200 mm^3. Three mice in the control group received intratumoral injection of 100 μL PBS per tumor, and three mice in the probe group received intratumoral injections of **PS-Q-NP** (50 μM/100 μL PBS/tumor). Mice in the GSH inhibition group received intraperitoneal injections of BSO (125 mg/kg body weight, once a day) for two days, and then received intratumoral injections of **PS-Q-NP** (50 μM/100 μL PBS/tumor). Near infrared (NIR) fluorescence images (λ_{ex} = 620/20 nm, λ_{em} = 670/40 nm) were obtained using the IVIS Lumina imaging system at 10 min, 3 h, and 24 h after injection.

11. ^{1}H-NMR and ^{13}C-NMR Spectra

^{1}H-NMR Spectrum of Compound **4** in $CDCl_3$ (400 MHz):

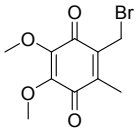

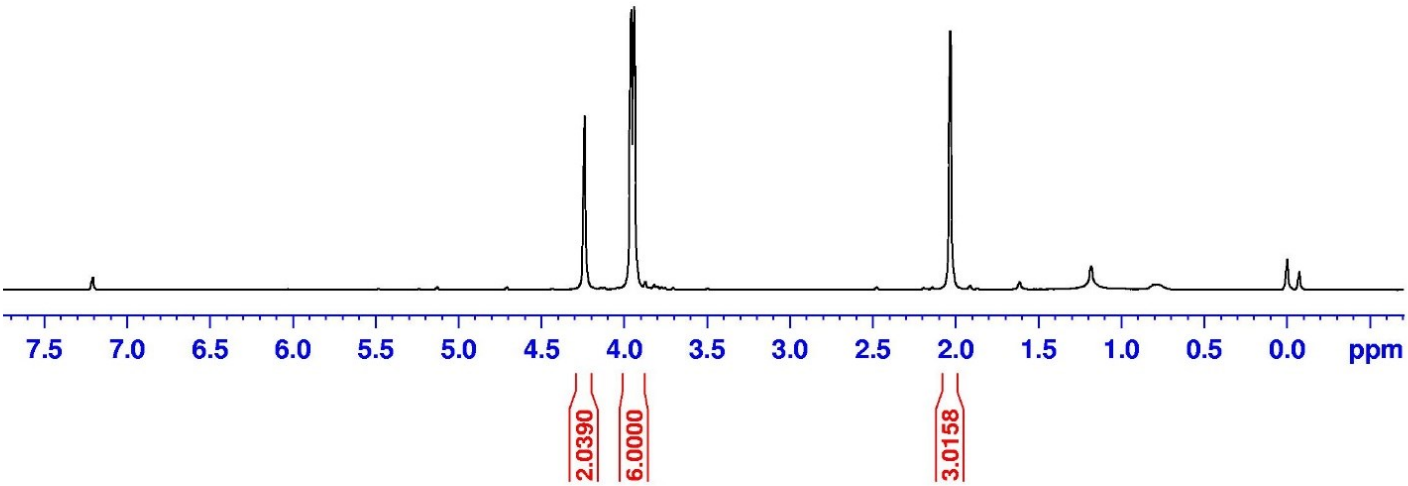

^{13}C-NMR Spectrum of Compound **4** in $CDCl_3$ (100 MHz):

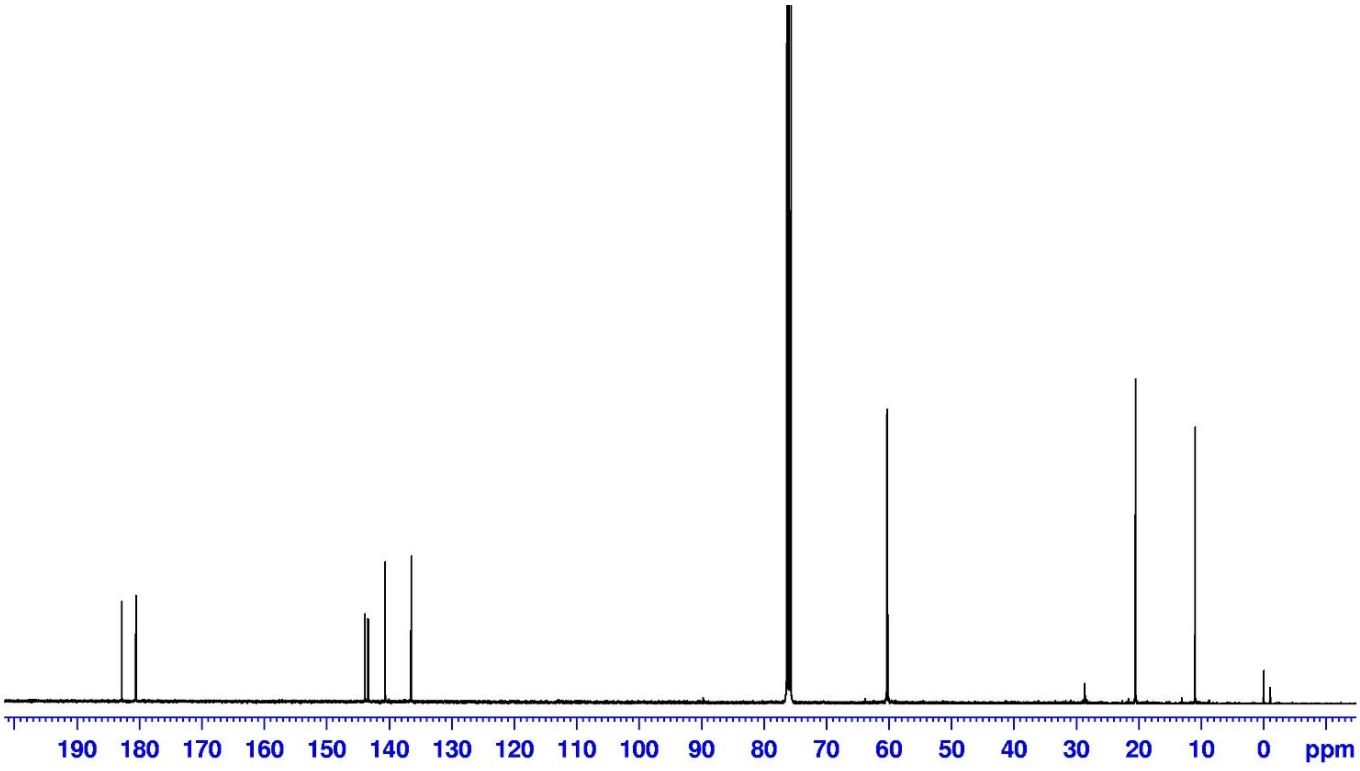

^{1}H-NMR Spectrum of Compound **2** in $CDCl_3$ (400 MHz):

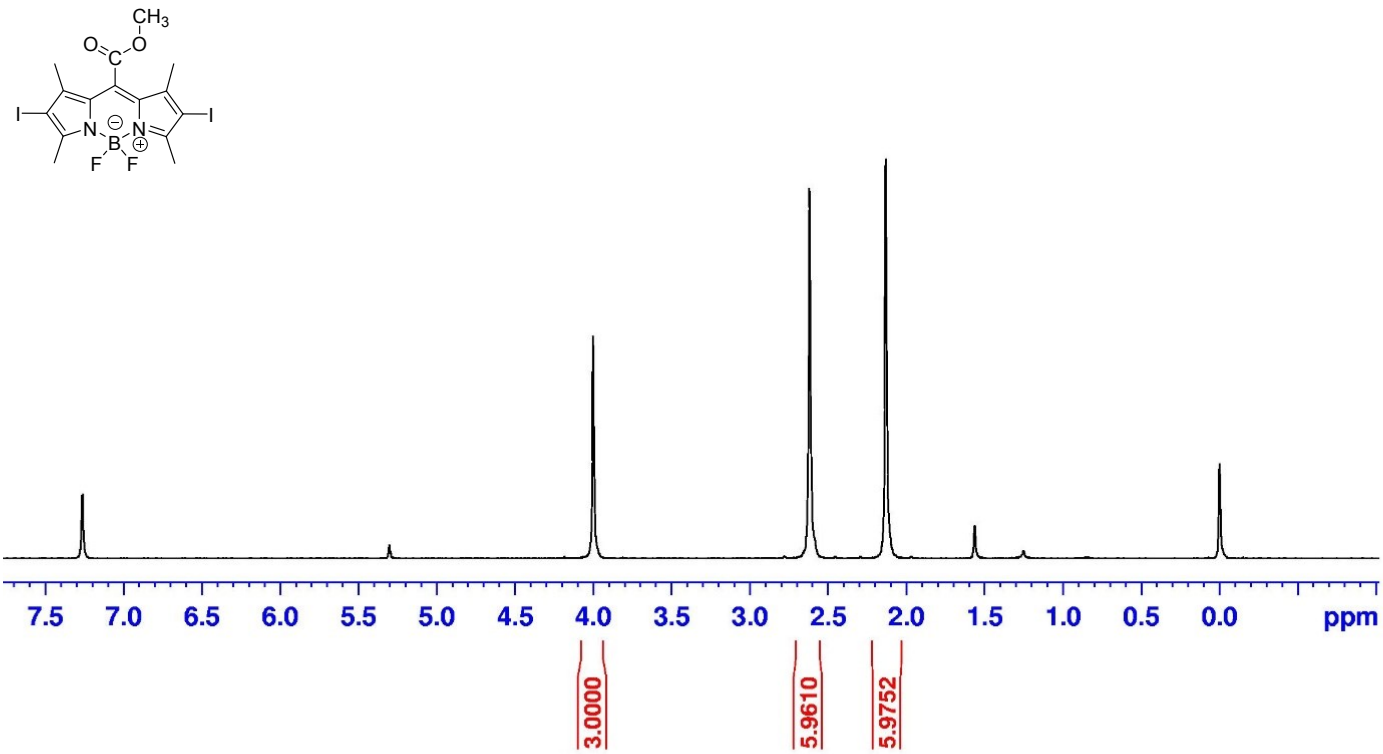

^{13}C-NMR Spectrum of Compound **2** in $CDCl_3$ (100 MHz):

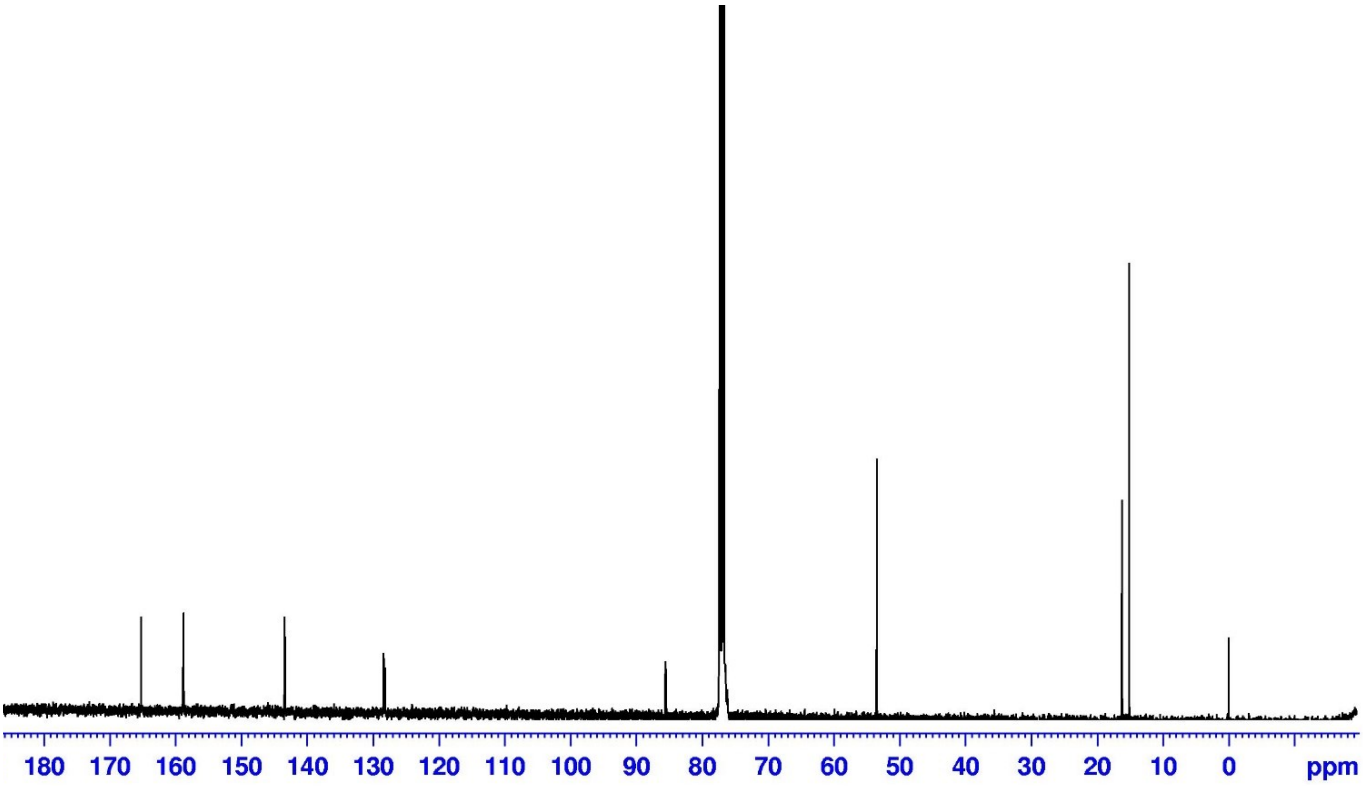

^{1}H-NMR Spectrum of **PS-E** in $CDCl_3$ (400 MHz):

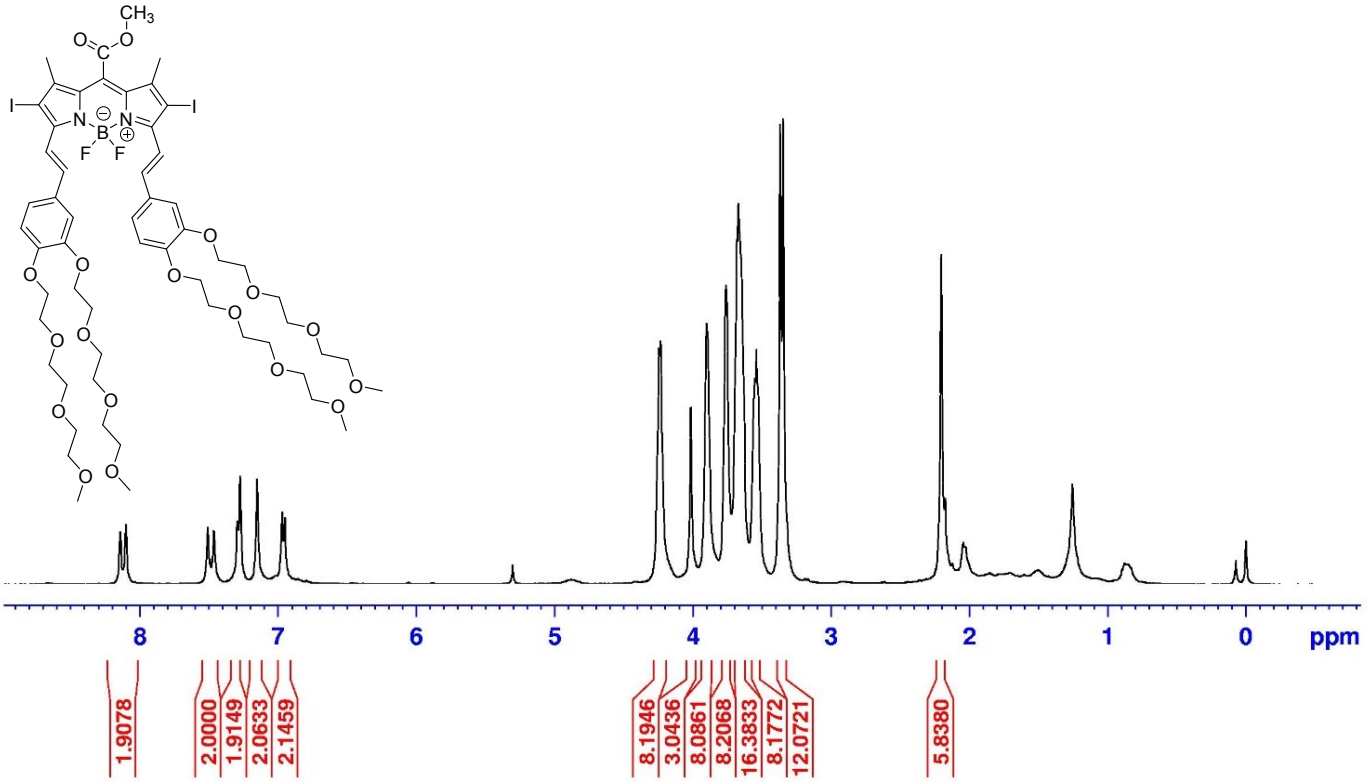

^{13}C-NMR Spectrum of **PS-E** in $CDCl_3$ (100 MHz):

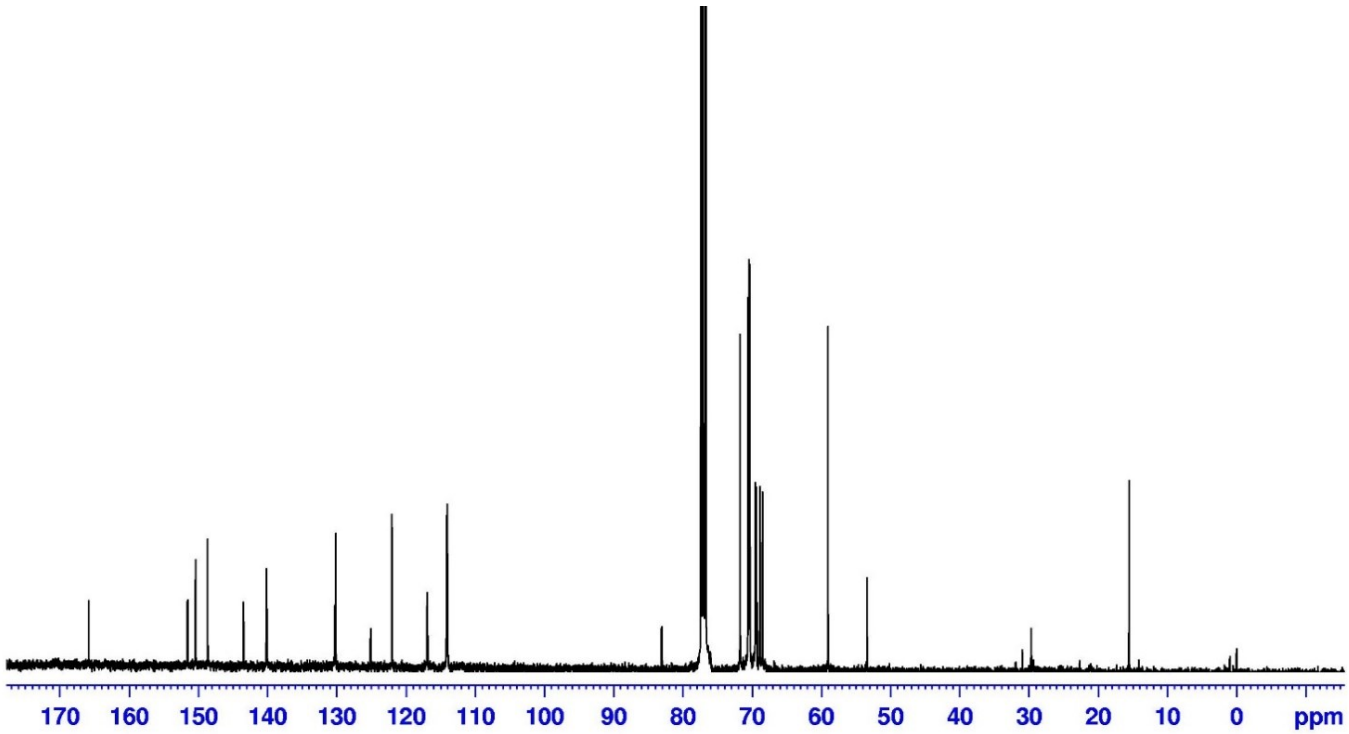

^{1}H-NMR Spectrum of **PS-A** in CD_3OD (400 MHz):

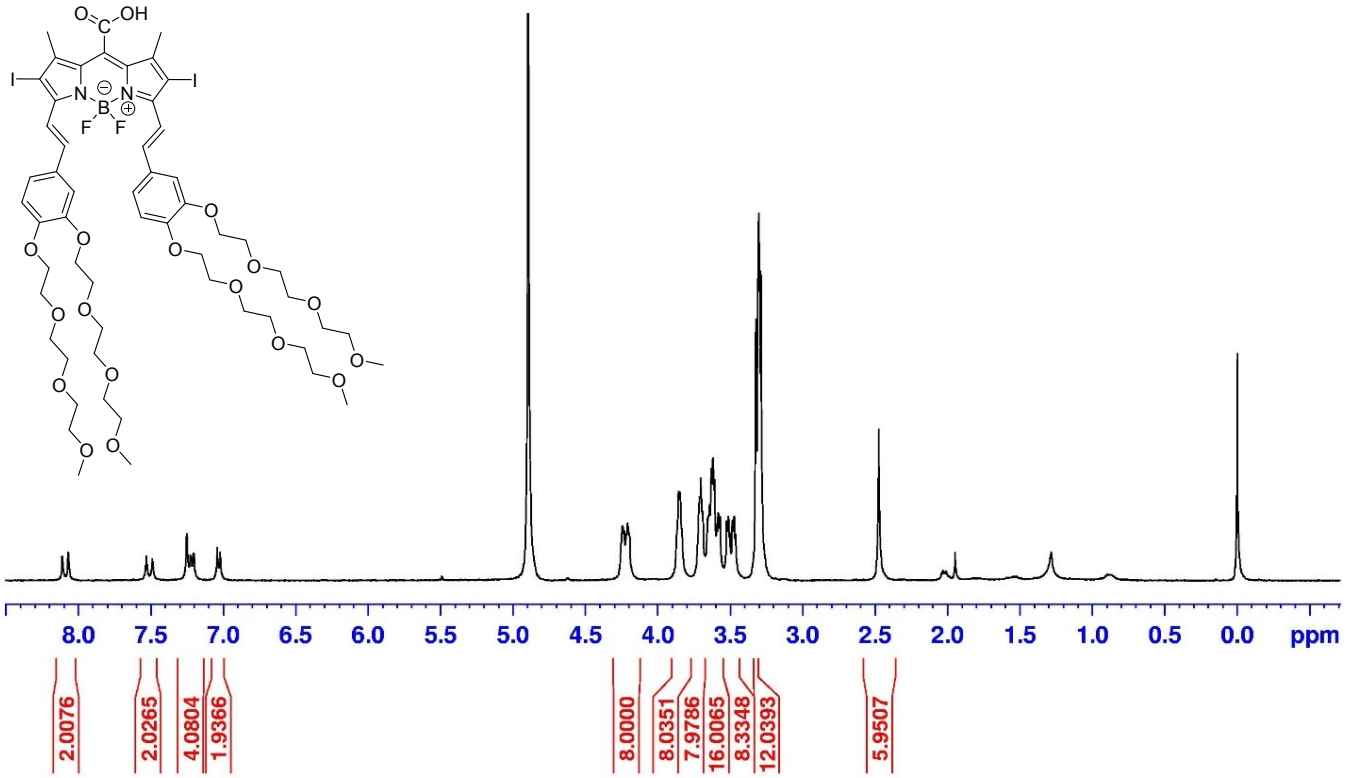

^{13}C-NMR Spectrum of **PS-A** in CD_3OD (100 MHz):

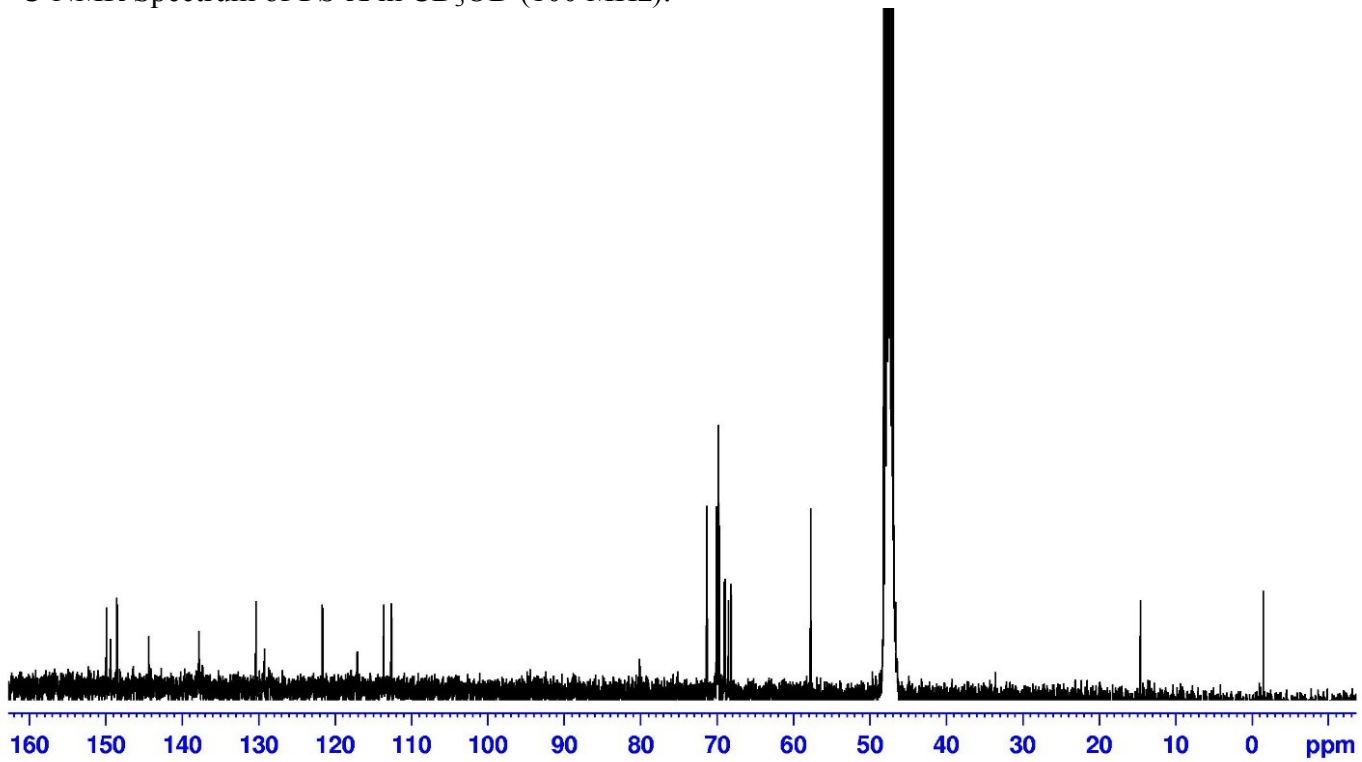

^{1}H-NMR Spectrum of **PS-Q** conjugate in $CDCl_3$ (400 MHz):

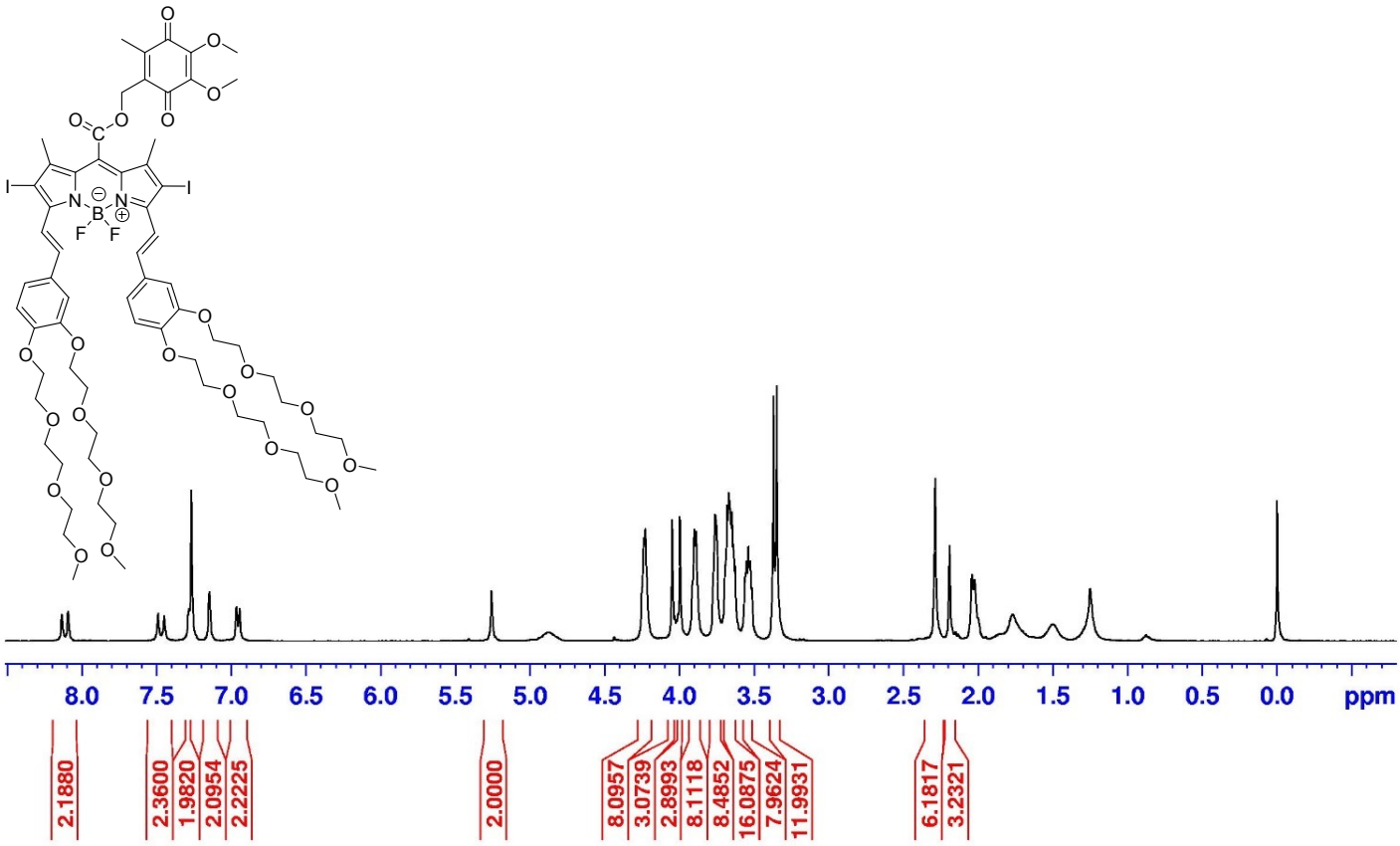

^{13}C-NMR Spectrum of **PS-Q** conjugate in $CDCl_3$ (100 MHz):

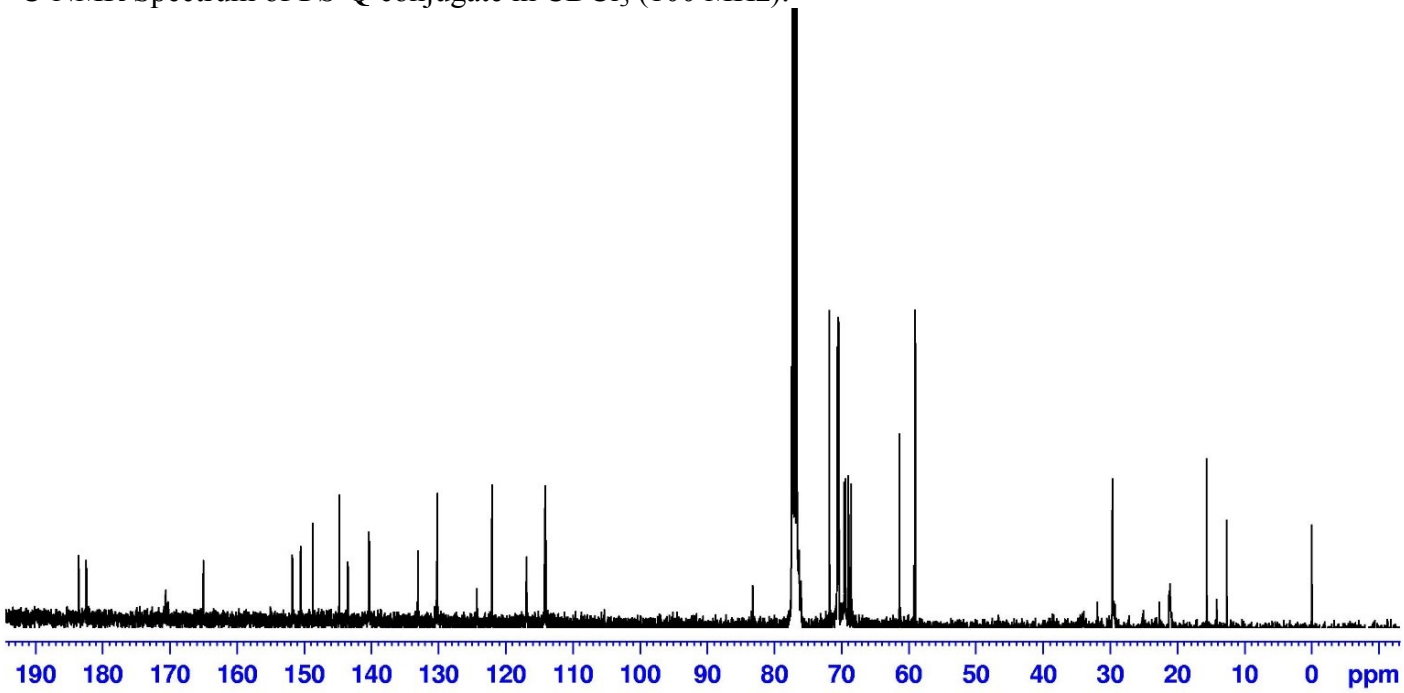

12. References

1. S. Kim, J. Bouffard and Y. Kim, *Chem. Eur. J.,* 2015, **21**, 17459.
2. B. H. Lipshutz, A. Lower, V. Berl, K. Schein and F. Wetterich, *Org. Lett.,* 2005, **7**, 4095.
3. G. Sargsyan, B. M. Leonard, J. Kubelka and M. Balaz, *Chem. Eur. J.,* 2014, **20**, 1878.
4. J. X. Duggan, J. DiCesare and J. F. Williams, New Directions in Molecular Luminescence, ed. D. Eastwood, ASTM International, Special Technical Publication 822, Philadelphia, 1983, pp. 112.
5. R. Sens and K. H. Drexhage, *J. Lumin.*, 1981, 24/25, 709.
6. K. Gollnick and A. Griesbeck, *Tetrahedron,* 1985, **41**, 2057.
7. (*a*) N. Adarsh, R. R. Avirah and D. Ramaiah, *Org. Lett.,* 2010, **12**, 5720; (*b*) H. S. Jung, J. Han, H. Shi, S. Koo, H. Singh, H.-J. Kim, J. L. Sessler, J. Y. Lee, J.-H. Kim and J. S. Kim, *J. Am. Chem. Soc.,* 2017, **139**, 7595.
8. X. Ragàs, A. Jimenez-Banzo, D. Sánchez-García, X. Batllori and S. Nonell, *Chem. Commun.,* 2009, 2920.
9. (*a*) R. W. Redmond and J. N. Gamlin, *Photochem. Photobiol.,* 1999, **70**, 391; (*b*) L. Xiao, L. Gu, S. B. Howell and M. J. Sailor, *Acs Nano,* 2011, **5**, 3651.
10. (*a*) O. W. Griffith and A. Meister, *J. Biol. Chem.*, 1979, **254**, 7558–7560; (*b*) O. W. Griffith, *J. Biol. Chem.*, 1982, **257**, 13704–13712; (*c*) A. Tagde, H. Singh, M. H. Kang and C. P. Reynolds, *Blood Cancer J.,* 2014, **4**, e229-e241.